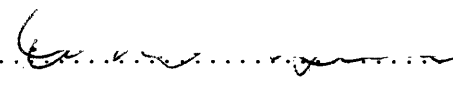# Quantum Spin Transport in Paramagnetic Systems

by

Daniel Greenbaum

Submitted to the Department of Physics
in partial fulfillment of the requirements for the degree of

Doctor of Philosophy

at the

MASSACHUSETTS INSTITUTE OF TECHNOLOGY

February 2005

Author . . . .
Department of Physics
October 12, 2004
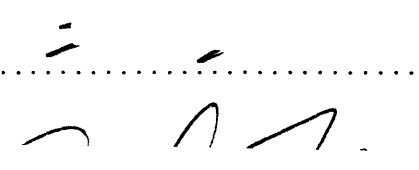
Certified by . . . .
David G. Cory
Professor
Thesis Supervisor
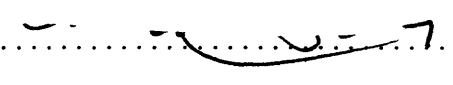
Certified by . . . .
Leonid S. Levitov
Professor
Thesis Supervisor
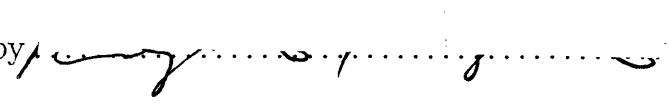
Read by . . . .
Edward H. Farhi
Professor
Thesis Reader

Read by . . . .
Raymond Ashoori
Professor
Thesis Reader

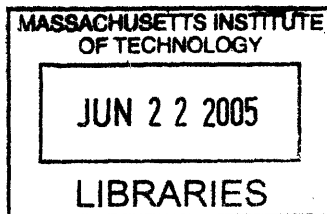Accepted by . . . .
Thomas J. Greytak
Associate Department Head for Education

ARCHIVES

Quantum Spin Transport in Paramagnetic Systems

by

Daniel Greenbaum

Abstract

We have studied the transport of magnetization and energy in systems of spins 1/2 on a lattice at high temperature. This work was motivated by recent experiments which observed "spin diffusion" among the dipolar coupled nuclear spins of the insulator calcium fluoride, under conditions where it was appropriate to neglect the coupling to any heat reservoir. The dynamics under these conditions is coherent and reversible, yet signatures of irreversibility (i.e. diffusion) are typically observed. This state of affairs poses a formidable conceptual puzzle. In this thesis we present both phenomenological and microscopic models of spin diffusion, retaining the important aspects of statistical approaches to transport while incorporating relevant quantum effects. These methods allow an efficient calculation of energy diffusion for a long-range interaction, which has largely been an intractable problem. We study transport in two different limits, that where the XY term of the spin Hamiltonian is dominant, and that where it can be treated as a perturbation compared to the Ising term. In the case of dipolar couping, both limits are found to show slightly more rapid diffusion of inter spin energy than magnetization, in qualitative agreement with experiments.

Thesis Supervisor: David G. Cory
Title: Professor

Thesis Supervisor: Leonid S. Levitov
Title: Professor

Acknowledgments

I would like to thank my advisor, Professor David Cory, for inviting me to join his research group two years ago. I am grateful to him for suggesting the problem described in this thesis and for much encouragement along the way. From David I learned many valuable lessons both about science and about how to communicate science effectively to other people. The work described in Chapter 3 was inspired by a conversation with Professor Leonid Levitov, and I am grateful to him both for that and for several other useful discussions over the past few years. A number these produced fresh ideas that made an important impact on my research.

I would like to thank Chandrasekhar Ramanathan for the many insights about NMR and spin dynamics that he shared with me, and Markus Kindermann for the many brilliant ideas that he contributed, which really helped to get the project off the ground. I would also like to thank the rest of the Cory group, Tatjana Atanasijevic, Nick Boulant, Greg Boutis, Paola Cappellaro, Debra Chen, Joon Cho, Joseph Emerson, Michael Henry, Jonathan Hodges, T. S. Mahesh, Dima Pushin, Suddha Sinha, and Jamie Yang, for many conversations both scientific and not, and for their friendship. Dima, Paola, and Jonathan also provided much appreciated help and input.

Many thanks go to the rest of the wonderful people I have met in my five years in graduate school, and whose friendship is what really made the experience worthwhile. Although I cannot list everyone here, I would like to thank in particular Gil Refael, Mukund Thattai, Andy Linshaw, Lynn Johnson, David Strozzi, and Darius Torchinsky, for freely offering their advice, support, and company in happy as well as challenging times. I am especially indebted to Larissa Duzhansky, since many of those happy times are thanks to her. Finally, I would like to thank my family for being my biggest supporters in whatever goals I wished to pursue, for helping me to battle the obstacles along the way, and for being the first to rejoice when they were overcome. To them I dedicate this thesis.

Contents

List of Figures

List of Tables

Chapter 1

Introduction

This thesis presents one aspect of recent theoretical work on the quantum dynamics of solid state spin systems at high temperature.[1] We will be concerned primarily with the spatial transport of magnetization and energy via mutual flips of spins that are fixed on the sites of a regular lattice. This is also known by the collective term "spin diffusion". In the systems where it has been observed, mainly the nuclear spins of insulators, it typically occurs on timescales that are shorter than those of relaxation mechanisms that decohere the wavefunction. In this regime, the dynamics cannot be diffusive in the strict sense of an incoherent, random process. Rather, the appearance of diffusion arises from a sort of quantum dephasing similar to that responsible for free induction decay. The dynamics in this case is entirely coherent, because the system is completely isolated and cannot at any time be considered to be in equilibrium with a heat bath. The physics of transport in such a system is of interest both at a fundamental and a practical level. Fundamentally, it is important to understand how the appearance of irreversibility arises despite the experimental ability to "reverse" the dynamics and produce an "echo" of the original state. (For dipolar coupled spins in solids an experimental technique to produce such an echo was demonstrated by Rhim, Pines and Waugh in 1971.[4]) On the practical side, one would like to add new controllable methods of transporting and storing complicated quantum states to the toolbox of quantum information processing.

---

[1]Parts of this thesis have been adapted from Refs. [1] and [3]

Our applications will be primarily to nuclear spins, because of their long decoherence times and the associated availability of experimental data. In contrast to electronic spins, whose magnetic moments are $\sim 10^3$ times larger than those of nuclei, nuclear spin-lattice relaxation times in solids can be as long as hours or minutes, allowing transport to take place. Because the transition rate due to spin-phonon coupling is proportional to γ^6, (see Ref. [5], Chapter 9) where γ is the gyromagnetic ratio, electronic spins thermalize much too rapidly for transport to be possible. Spin diffusion was originally found to occur in insulating salts such as calcium fluoride, where the Fluorine atoms have nuclear spin 1/2 and therefore no quadrupole moment, so that dipolar coupling is the main interaction. However, it has also been observed in other systems, most notably the exchange-coupled nuclear spins of solid ^{3}He.[6, 7] Because of their accessibility to manipulation by NMR methods, and the importance of their interactions with electrons in solid-state devices, nuclear spins have also been at the center of attention in recent efforts to implement quantum computation. (see, e.g. Refs. [8, 9, 10, 11]) Lately there has also been a flurry of studies of spin diffusion in spin chains, but we will not discuss these here. See, e.g. [12], and references therein.

We focus on high temperature systems both because we expect statistical methods to work in this case, and because the relevant experiments have been carried out in this regime. Because of the coherence of the transport process, the words "temperature" and "equilibrium" should be used with caution. In practice, experiments are typically carried out on systems that have been allowed to come to a genuine equilibrium at a very high temperature, so that the initial state is one of spins pointing in nearly random directions. In NMR experiments, this means that the crystal is placed in an external field for a time much longer than the spin-lattice relaxation time, T_1, so that a small equilibrium magnetization is produced. This magnetization can be considered as a perturbation on the infinite temperature state of completely random spin orientations (or equal occupation probabilities of the Zeeman levels). The residual equilibrium magnetization can be driven out of equilibrium in order to produce transport. Because of the coherence of the process, the system retains memory of

its initial state, and the notion of equilibrium during transport is meaningless. It is therefore proper to use the term "high temperature" only in connection with the ensemble from which the initial state is taken. If the same experiment is repeated many times, however, it then becomes possible to think of the *average* transport coefficients over all realizations of the experiment. In this sense we expect a statistical theory to be valid.

Our investigations are therefore geared towards learning whether there are any uniquely quantum manifestations of the coherence that are universal in the sense of being independent of the particular starting state. One can imagine, for example, the interference of paths along which a spin can diffuse, that would affect the value of the diffusion coefficient regardless of which state it started in. A hint to the existence of such processes has recently been reported[1] in connection with the measurement of an anomalously large value for the energy diffusion coefficient in calcium fluoride. To determine whether such phenomena really exist requires a fully quantum-mechanical treatment of the problem. This is the goal of this thesis.

In this thesis we present calculations of correlation functions and diffusion coefficients in two different limits. The first limit is when the flip-flop (I^+I^-) interaction is dominant over all other interactions. This is known as the XY model, and is the simplest model exhibiting spin diffusion. It is an important starting point for determining the effect of other interactions. The second limit is that of a general bilinear spin-conserving interaction for which the flip-flop can be treated in perturbation theory. Each limit lends itself to analysis by a different technique in order for a solution to be possible or for the calculations to be tractable. Our primary tools are Redfield's moment method and linear response theory. Using the former, we obtain the diffusion coefficients of both magnetization and energy for the XY model with arbitrary coupling in Chapter 2. Next, in Chapter 3, we prove the equivalence of the diffusion coefficients obtained from an equation of motion analysis of the correlation function to those given by Kubo's formula. We use the latter as a basis for a perturbation expansion in the flip-flop term.

In this chapter, we present a qualitative physical discussion of spin diffusion,

including Bloembergen's original phenomenological theory. A discussion is given of the reciprocal space NMR method that was recently used to measure magnetization and energy autocorrelation functions for the nuclear spins in calcium fluoride. These experiments provided the first direct measurements of these quantities in an isolated dipolar coupled spin system, and showed that energy diffusion is several times faster than expected from quasi-classical considerations, while magnetization diffusion is well described classically. After establishing formulas for the measured quantities, we give a simple argument for why a coherently evolving system may display significantly different behavior than a dissipative one. Finally, a review is given of previous work on this problem.

1.1   Lattice Spin Systems

The most general Hamiltonian for a set of spins on a rigid lattice with only pairwise interactions, and conserving at least one component of spin, is

$$\mathcal{H} = \sum_{i,j}^{N} \left(A_{ij} I_i^z I_j^z + B_{ij} I_i^+ I_j^- \right), \tag{1.1}$$

where N is the total number of spins in the crystal. The latin indices run over all lattice sites and the I_i^α are spin operators defined by their commutation relations $[I_i^\alpha, I_j^\beta] = \delta_{ij} I_i^\gamma$, where α, β, γ is any cyclic permutation of x, y, z. The $I_j^\pm \equiv I_j^x \pm i I_j^y$ are raising and lowering operators. The important feature of Eq. (1.1) is the "flip-flop" term, $\sum_{i,j} B_{ij} I_i^+ I_j^-$, which is responsible for the transport of magnetization and energy (or heat) by the mutual flips of pairs of spins. Eq. (1.1) includes the models of interest for spin diffusion as special cases: (1) Heisenberg model, for which A_{ij}, B_{ij} are non-zero for $|\mathbf{r}_i - \mathbf{r}_j| = 1$ and are zero otherwise. This model is appropriate for nuclear spin diffusion in ^{3}He. Also, $A_{ij} = B_{ij}$ for the isotropic Heisenberg model; (2) XY-model, where $A_{ij} = 0$ and B_{ij} is arbitrary. We study this model in Chapter 2; and (3) dipolar coupling in high external magnetic field, for which $B_{ij} = -\frac{1}{2} A_{ij}$, and

$A_{ij} = b_{ij}$, where

$$b_{ij} = \frac{\gamma^2 \hbar}{2} \frac{1 - 3\cos^2\theta_{ij}}{r_{ij}^3}. \tag{1.2}$$

Here γ is the nuclear gyromagnetic ratio, $\mathbf{r}_{ij}$ is the displacement between lattice sites i and j, and θ_{ij} is the angle between $\mathbf{r}_{ij}$ and the external magnetic field $\mathbf{B}_0$, which is taken to lie along the z-axis. Model (3) is directly applicable to nuclear spins in insulating solids, and is important for any magnetic system in an external field, since the dipolar coupling between spins is always present regardless of other interactions. In all sums over several indices, it will be understood that no two indices are the same, or equivalently, we set $A_{ii} = 0 = B_{ii}$.

The case of dipolar coupling requires special consideration, since the dipolar interaction without external field does not conserve any component of the total spin. In an external magnetic field which produces a Zeeman splitting between neighboring levels that is much larger than the interaction strength between any pair of spins, transitions which change the total component of spin along the field are suppressed compared to spin-conserving transitions, due to energy conservation. This results in an effective truncation of the full dipolar-coupling. This fact is well known in the NMR community,[13] but is not widely appreciated. For completeness, we present a detailed discussion here.

1.1.1 Dipolar coupling in strong external field

A system of identical dipolar-coupled spins in a constant external magnetic field, $\mathbf{B}_0$, has the Hamiltonian $\mathcal{H} = \mathcal{H}_Z + \mathcal{H}_{dip}$, where[5, 13]

$$\mathcal{H}_Z = -\sum_i \mathbf{m}_i \cdot \mathbf{B}_0, \tag{1.3}$$

$$\mathcal{H}_{dip} = \frac{1}{2}\sum_{i,j}\left[\frac{\mathbf{m}_i \cdot \mathbf{m}_j}{r_{ij}^3} - \frac{3\,(\mathbf{m}_i \cdot \mathbf{r}_{ij})\,(\mathbf{m}_j \cdot \mathbf{r}_{ij})}{r_{ij}^5}\right]. \tag{1.4}$$

The factor $\frac{1}{2}$ in Eq. (1.4) compensates for counting each term twice in the sum. The magnetic moment operator at site i is proportional to the spin operator at that site, $\mathbf{m}_i = \gamma\hbar\mathbf{I}_i$, and $\mathbf{r}_{ij} \equiv \mathbf{r}_i - \mathbf{r}_j$ is the displacement vector between sites i and j.

We may treat $\mathcal{H}_{dip}$ as a perturbation if the "local field", $B_{loc} \equiv \gamma\hbar/a^3$, satisfies $B_{loc} \ll B_0$, where a is the lattice constant. This condition is typically satisfied for nuclear spins in experimentally accessible external fields. For the Fluorines of calcium fluoride at an external field of 1-10 T, we have $B_{loc}/B_0 \sim 10^{-4}$. The unperturbed energy levels are simply the Zeeman levels of an assembly of spins in the field $\mathbf{B}_0$, and the dipolar interaction causes transitions between them. These transitions are most easily analysed by writing the dot products in Eq. (1.4) in component form, and expressing I_i^x and I_i^y in terms of the raising and lowering operators, $I_i^{\pm} = I_i^x \pm iI_i^y$. Also, the displacement vectors between lattice sites are conveniently written in polar coordinates, $\mathbf{r}_{ij} = r_{ij} \times (\sin\theta_{ij}\cos\phi_{ij}, \sin\theta_{ij}\sin\phi_{ij}, \cos\theta_{ij})$, with the polar axis along the external field. This gives

$$\mathcal{H}_{dip} = \frac{\gamma^2\hbar^2}{2}\sum_{i,j}\frac{A_{ij} + B_{ij} + C_{ij} + D_{ij} + E_{ij} + F_{ij}}{r_{ij}^3} = \mathcal{H}_A + \cdots + \mathcal{H}_F, \qquad (1.5)$$

where

$$
\begin{aligned}
A_{ij} &= I_i^z I_j^z (1 - 3\cos^2\theta_{ij}), \\
B_{ij} &= -\frac{1}{4}(I_i^+ I_j^- + I_i^- I_j^+)(1 - 3\cos^2\theta_{ij}), \\
C_{ij} &= -\frac{3}{2}(I_i^+ I_j^z + I_i^z I_j^+)\sin\theta_{ij}\cos\theta_{ij}e^{-i\phi_{ij}}, \\
D_{ij} &= -\frac{3}{2}(I_i^- I_j^z + I_i^z I_j^-)\sin\theta_{ij}\cos\theta_{ij}e^{i\phi_{ij}}, \\
E_{ij} &= -\frac{3}{4}I_i^+ I_j^+ \sin^2\theta_{ij}e^{-2i\phi_{ij}}, \\
F_{ij} &= -\frac{3}{4}I_i^- I_j^- \sin^2\theta_{ij}e^{2i\phi_{ij}}. \qquad (1.6)
\end{aligned}
$$

The terms A_{ij} and B_{ij} have their only matrix elements between unperturbed levels of the same energy. In particular, A_{ij} is diagonal in the product basis, $\{|m_1, m_2, \ldots, m_N\rangle = |m_1\rangle \otimes |m_2\rangle \otimes \cdots \otimes |m_N\rangle\}$, where m_i is the spin quantum number along the external field. B_{ij} connects the pair of states $|\ldots, m_i, \ldots, m_j+1, \ldots\rangle, |\ldots, m_i+1, \ldots, m_j, \ldots\rangle$ as well as a similar pair with i and j interchanged. The remaining terms connect levels of different energy. Therefore, in the absence of any other perturbing fields (such

as an rf excitation) only transitions caused by $\mathcal{H}_A$ and $\mathcal{H}_B$ conserve energy. The remaining terms in the dipolar Hamiltonian cannot cause any transitions if the spacing between Zeeman levels is larger than the width of the density of states at each level. The ratio of this width to the Zeeman energy spacing is of order B_{loc}/B_0, which is in practice much smaller than one. The rate of such transitions is therefore zero by Fermi's golden rule.

Another way to see this is by time-independent perturbation theory. Let $\{|n_m^{(0)}\rangle\}$ denote the basis of unperturbed eigenfunctions in which the terms $\mathcal{H}_A$ and $\mathcal{H}_B$ are diagonal. The label n denotes a given Zeeman energy, and each level within the degenerate subspace at a given energy is labelled by the subscript m. To first order, the energy levels are therefore $E_{nm} = E_n^{(0)} + E_{nm}^{(1)}$, where $E_{nm}^{(1)} = \langle n_m^{(0)}|\mathcal{H}_A + \mathcal{H}_B|n_m^{(0)}\rangle \sim \gamma\hbar B_{loc}$. Since the terms C_{ij} through F_{ij} have no diagonal elements in this basis, they produce no change in the energy levels at first order. The second order energy shift is

$$E_{nm}^{(2)} = \sum_{n',m'(n'\neq n; m'\neq m)} \frac{|\langle n_m^{(0)}|\mathcal{H}_C + \cdots + \mathcal{H}_F|n'_{m'}^{(0)}\rangle|^2}{E_n^{(0)} - E_{n'}^{(0)}}. \tag{1.7}$$

Since the matrix elements in Eq. (1.7) connect neighboring and next-neighboring Zeeman levels, we have $E_{nm}^{(2)} \sim \gamma\hbar B_{loc}(B_{loc}/B_0)$. Likewise, the correction to the unperturbed eigenfunctions is solely due to $\mathcal{H}_C, \ldots, \mathcal{H}_F$, and is also of order B_{loc}/B_0. As mentioned above, we typically have $B_{loc}/B_0 \ll 1$ in experimental situations of interest. Therefore the dependence of the energies and eigenfunctions on the terms $\mathcal{H}_C, \ldots, \mathcal{H}_F$ is unobservable in practice. This has been checked experimentally by NMR spectroscopy for various systems, which has shown the near vanishing of the intensities of resonances between non-neighboring Zeeman levels.[5, 13] (Since the rf Hamiltonian connects only those Zeeman levels neighboring in energy, transitions between other levels are higher-order effects due to the terms $\mathcal{H}_C, \ldots, \mathcal{H}_F$.)

The above arguments allow us to truncate the dipolar Hamiltonian of Eq. (1.4), resulting in

$$\mathcal{H}_{dip}^{(0)} = \sum_{i,j} b_{ij} \left(I_i^z I_j^z - \frac{1}{4}\left(I_i^+ I_j^- + I_i^- I_j^+\right)\right), \tag{1.8}$$

with b_{ij} given by Eq. (1.2). We mention that, despite the coupling to the external field, Eq. (1.3), we may neglect this field and consider Eq. (1.8) to be the full Hamiltonian for dipolar coupling, since a transformation to a rotating coordinate system is sufficient to eliminate the Zeeman energy term.

1.2 Spin Diffusion Phenomenology

Spin diffusion was first suggested by Bloembergen to explain his experiments on spin-lattice relaxation in various insulating salts, including calcium fluoride.[14] He found that the relaxation times varied by orders of magnitude between samples. In his theory, spin-lattice relaxation was caused by diffusion of nuclear magnetization to rapidly relaxing paramagnetic impurities, whose concentration varied from sample to sample. Bloembergen proposed a simple, phenomenological model which accounted rather well for the order of magnitude of the relaxation rate, but was limited in some important ways. His model is presented here, followed by a discussion in the next section of later developments which stemmed from it.

Bloembergen assumed a system of spins $\frac{1}{2}$ on a lattice where nearest neighbor spins could flip with each other with probability W per unit time. It is easy to show that the magnetization of this system obeys a diffusion equation.[5, 14] Consider a chain of such spins, spaced by a distance a. The rate of change of the probability, $p_+(x, t)$, that a spin is up at position x and time t, is

$$\frac{1}{W}\frac{\partial p_+(x)}{\partial t} = p_-(x)[p_+(x+a) + p_+(x-a)] - p_+(x)[p_-(x+a) + p_-(x-a)]. \quad (1.9)$$

A similar equation holds for $p_-(x, t)$, the probability that a spin is down at x and t. Writing $p_+ - p_- = p$, $p_+ + p_- = 1$, and assuming $p \ll 1$, so that terms quadratic in p are negligible, we obtain

$$\frac{\partial p(x)}{\partial t} = W[p(x+a) + p(x-a) - 2p(x)]. \quad (1.10)$$

This is the finite difference form of the diffusion equation. To see this, one can expand

the right hand side in Taylor series and keep only the lowest order terms. This gives

$$\frac{\partial p}{\partial t} = Wa^2 \frac{\partial^2 p}{\partial x^2}.$$ (1.11)

The above argument is generalizable to three dimensions. If we neglect the anisotropy of W, we obtain

$$\frac{\partial p}{\partial t} = D\nabla^2 p,$$ (1.12)

where $D = Wa^2$. If W is anisotropic, the diffusion rate becomes dependent on direction, and $D\nabla^2$ is replaced by $\sum_{ij} D_{ij}\partial_i\partial_j$, where D_{ij} is the diffusion tensor.

The magnitude of D can be estimated using Fermi's golden rule. From Eq. (1.1), the matrix element between any two states differing only by a flipped pair of nearest neighbor spins is $\langle + - |\mathcal{H}| - + \rangle = -b/2$, where $b = b_{ij}$ for i and j nearest neighbors. Treating the dipolar interaction as a perturbation at zero frequency, one obtains

$$W = \frac{\pi}{2\hbar^2}|b|^2\delta(\omega_i - \omega_f)f(\omega_i)f(\omega_f),$$ (1.13)

where the subscripts i and f denote initial and final states, and the density of states, $f(\omega)$, is given by the free induction decay lineshape. (The lineshape is simply the distribution of precession frequencies caused by the dipolar interaction, which is the same as the energy distribution of a single spin.) Assuming a gaussian lineshape with width $\Delta\omega$ and integrating over all initial and final states, we obtain

$$W = \frac{\pi}{2\hbar^2}\frac{b^2}{\sqrt{2\pi(\Delta\omega)^2}}.$$ (1.14)

A formula for $\Delta\omega$ in terms of the couplings, b_{ij}, has been obtained by Van Vleck[15] by a moment method. For a simple cubic lattice, this formula is[5]

$$\Delta\omega^2 = 12.3\gamma^4\hbar^2 I(I+1)\frac{1}{a^6}(\lambda_1^4 + \lambda_2^4 + \lambda_3^4 - 0.187),$$ (1.15)

where I is the magnitude of the spin and λ_1, λ_2, λ_3 are the direction cosines of the applied field with respect to the crystal axes. For $I = 1/2$, and the crystal oriented

such that one of the crystal axes is along the external field (say, the [001] direction) we obtain

$$W_{\parallel}(001) \;=\; (0.229)\frac{\gamma^2 \hbar}{a^3}, \tag{1.16}$$

$$W_{\perp}(001) \;=\; \frac{1}{4}W_{\parallel}(001), \tag{1.17}$$

where the subscript $\parallel$ means nearest neighbors on an axis parallel to $\mathbf{B}_0$, and the subscript $\perp$ denotes nearest neighbors perpendicular to $\mathbf{B}_0$. This shows that the longitudinal diffusion coefficient, $D_{\parallel}$, for transport along the direction of the external field is greater than the transverse diffusion coefficient, $D_{\perp}$, for transport perpendicular to the field. In this thesis, we will only be concerned with calculating $D_{\parallel}$. For the Fluorines in calcium fluoride, the values of the constants are $\gamma = 2.51 \times 10^4$ rad Hz/Oe, $a = 2.73 \times 10^{-8}$ cm. Putting these values in the above equation, we obtain an estimate for $D_{\parallel}$ of 5.5×10^{-12} cm^2 s^{-1}, which is remarkably close to the experimentally measured value (see Table 1.1).

Experiments are typically done for two different orientations of the field with respect to the crystal axes, the (001) and (111) directions. Two orientations are sufficient to compare with theory. However, obtaining a good estimate from the above theory of $D_{\parallel}$ for the (111) direction is difficult because nearest neighbors no longer contribute to the transport (they have $b = 0$), and we must consider various ways of producing longitudinal transport by flip-flops of next-nearest neighbors. The approximation is then too qualitative and does not give reasonable results. Furthermore, there is no clear way to estimate the rate of energy transport using this theory. However, the more detailed theories we describe later do predict an orientation dependence of the diffusion coefficient that is close to what is measured experimentally, and also provide a way to calculate energy transport.

1.3 Reciprocal Space NMR Technique

The experiments of Zhang and Cory[2] and Boutis, et al.[1] provided a measurement of the spin-spin and energy-energy correlation functions in Fourier space for the spin 1/2 Fluorine nuclei in calcium fluoride. They were carried out at room temperature, using pulsed gradient NMR techniques. In these experiments, a single crystal of calcium fluoride was first allowed to reach thermal equilibrium in a strong external magnetic field, so that the initial population of spins pointed along the field was different than that of the ones pointed oppositely. The resulting polarization was manipulated with radio frequency (rf) pulses and magnetic field gradients in order to produce inhomogeneous magnetization and energy distributions whose coherent evolution under the dipolar coupling was measured. The evolution times were short compared to the spin-lattice relaxation time, T_1, but long compared to the spin-spin dephasing time, T_2. The dynamics was therefore coherent in the sense that the spin system was well isolated and was not relaxed by coupling to a thermal reservoir, while the evolution time was still long enough to accommodate many spin flips. The same experiment was carried out many times for single wavelength modulations between $1-3$ μm of the magnetization and energy densities. The results are reproduced in Table 1.1.

Since this thesis is concerned with theory, we will here describe how the experiment works *in principle*, and refer the reader to the original articles for details on the apparatus and implementation.[2, 1] The discussion of this section will be used as a framework for the theoretical developments presented later.

At thermal equilibrium in a strong external field, the density matrix of the spin system is of the form $\rho_{eq} = \frac{1}{Z} + \delta\rho$, where Z is the partition function and

$$\delta\rho \propto \sum_{i=1}^{N} I_z^i = I_z. \tag{1.18}$$

This state is known in the NMR community as "Zeeman order", and is created simply by leaving the crystal in the external magnetic field for a time long compared to the spin-lattice relaxation time. Indeed, in the high-field ($\gamma B_0 >> b_{ij} \ \forall \ i,j$), high-

Table 1.1: Summary of the experimental results of Refs. [1, 2] on the spin diffusion rate of spin-spin energy, $D_\mathcal{H}$, and magnetization, $D_\mathcal{M}$ for a single crystal of calcium fluoride in two different orientations ([001] and [111]) with respect to the external field.

Ref. [1]		[001]	[111]	D_{001}/D_{111}
$D_\mathcal{H}$	$(\times 10^{-12}\mathrm{cm}^2/\mathrm{s})$	29 ± 3	33 ± 4	0.88 ± 0.14
$D_\mathcal{M}$	$(\times 10^{-12}\mathrm{cm}^2/\mathrm{s})$	6.4 ± 0.9	4.4 ± 0.5	1.45 ± 0.26
Ref. [2]		[001]	[111]	D_{001}/D_{111}
$D_\mathcal{H}$	$(\times 10^{-12}\mathrm{cm}^2/\mathrm{s})$	7.1 ± 0.5	5.3 ± 0.3	1.34 ± 0.12
Ratio of $D_\mathcal{H}$ to $D_\mathcal{M}$		[001]	[111]	
Ref. [1]		4.5 ± 0.8	7.5 ± 1.3	−

temperature ($\gamma \hbar B_0 << k_B T$) limit, the equilibrium density matrix is[13]

$$\rho_{eq} = \frac{e^{-\mathcal{H}/(k_B T)}}{Z} \approx \frac{1}{Z}\left(\mathbf{1} - \frac{1}{k_B T}\mathcal{H}_Z\right) = \frac{1}{Z}\left(\mathbf{1} + \frac{\gamma \hbar B_0}{k_B T} I_z\right), \qquad (1.19)$$

where $\mathbf{1}$ is the identity operator and $Z = \mathrm{tr}\{\mathbf{1}\} = 2^N$ in this approximation. This density matrix describes a system with uniform infinitesimal polarization in the z-direction. Using the previously quoted value for γ in calcium fluoride, as well as typical values of $B_0 = 1$ T, $T = 300$ K, we estimate $\gamma \hbar B_0/k_B T \sim 10^{-5} - 10^{-6}$.

1.3.1 Magnetization diffusion experiment

The experiment begins with a $(\pi/2)_y$ pulse[2] applied to the state, Eq. (1.19), followed by a magnetic field gradient pulse sequence. This sequence consists of strong magnetic field gradient pulses along the z-axis, interleaved in the long delay times within a magic-echo train. The magic-echo train is a pulse sequence, demonstrated by Rhim, Pines, and Waugh,[4] which suspends evolution under the dipolar coupling. The combination of the magic echo and magnetic field gradient produces an effective

---

[2]This is the customary notation used in the NMR literature. $(\pi/2)_y$ stands for a 90 degree rf pulse about the y-axis, whose effect can be expressed mathematically by the application of the unitary operator $U((\pi/2)_y) = \exp(-i\frac{\pi}{2}I_y)$ to the state.

Hamiltonian consisting of just the gradient term,

$$\mathcal{H}_\nabla = \gamma \hbar \frac{\partial B_z}{\partial z} \sum_i I_i^z z_i, \tag{1.20}$$

where $\partial B_z/\partial z$ is the gradient field strength and z_i is the spatial location of spin i. This creates a spatially modulated magnetization transverse to the external field. If the gradient is applied for a total time δ, the wave number of the resulting spatial modulation is $k = \gamma \delta (\partial B_z/\partial z)$. Following the application of the gradient,

$$\delta \rho = \frac{\hbar \omega}{k_B T Z} \sum_i \left[I_i^x \cos(kz_i) + I_i^y \sin(kz_i) \right]. \tag{1.21}$$

Next, a $(\pi/2)_{\bar{y}}$ pulse flips one component of the transverse magnetization back along the external field (z axis). The remaining transverse component decays rapidly because it is not a conserved quantity (unlike the z component of the magnetization, which satisfies a local continuity equation as we will see in Chapter 3). This yields

$$\delta \rho = \frac{\hbar \omega}{k_B T Z} \sum_i I_i^z \cos(kz_i) \tag{1.22}$$

These steps are common to both the magnetization and energy diffusion experiments. For the measurement of magnetization diffusion, the above state is allowed to evolve under the Hamiltonian, Eq. (1.8), for a time t. Following this,

$$\delta \rho(t) = \frac{\hbar \omega}{k_B T Z} \sum_{ij} c_{ij}(t) I_j^z \cos(kz_i), \tag{1.23}$$

where the coefficients $c_{ij}(t)$ are infinite temperature spin-spin correlation functions,

$$c_{ij}(t) = \frac{\langle I_i^z(0) I_j^z(t) \rangle}{\langle (I_i^z)^2 \rangle}, \tag{1.24}$$

and $I_j^z(t) \equiv \exp(i\mathcal{H}t) I_j^z \exp(-i\mathcal{H}t)$ is the time-dependent spin operator in the Heisenberg picture. The angular brackets stand for the infinite temperature equilibrium average, $\langle \cdots \rangle \equiv \mathrm{tr}\{\cdots\}/\mathrm{tr}\{\mathbf{1}\}$. The c_{ij}'s represent the relative amount of polar-

ization initially at site i that has been transported to site j after time t. Because of translational invariance, they only depend on the vector difference $\mathbf{r}_i - \mathbf{r}_j$. We have neglected higher order spin terms in Eq. (1.23), as these do not contribute to a measurement of the magnetization.

Next, a $(\pi/2)_y$ pulse is applied followed by a magnetic field gradient, equal in amplitude but reversed in direction compared to the initial step. This gradient labels the new location of the polarization, in analogy with a scattering experiment. After a final $(\pi/2)_{\bar{y}}$ pulse, the state is

$$\delta\rho(t+0) = \frac{\hbar\omega}{k_B T Z} \sum_{i,j} c_{ij}(t) I_j^z \cos(kz_i)\cos(kz_j). \tag{1.25}$$

In the absence of spin diffusion, $c_{ij} = \delta_{ij}$, so that the phase terms would be identical and the original state would be recovered (scaled by 1/2 due to the dephasing of transverse spin components). In the presence of spin diffusion, the cosine terms reflect the spatial transport of the magnetization.

Finally, the total z magnetization of the state in Eq. (1.25) is measured. The signal, normalized to one when the evolution time is zero, will be denoted by $c_{\mathcal{M}}(k,t)$. It is equal to the expectation value of the magnetization in the final state, Eq. (1.25), divided by that in the same state at $t = 0$, or $\operatorname{tr}\{I^z \delta\rho(t+0)\}/\operatorname{tr}\{I^z \delta\rho(0+0)\}$. This can be rewritten in terms of infinite temperature equilibrium averages as

$$c_{\mathcal{M}}(k,t) = \frac{\langle \sum_i I_i^z(0)\cos(kz_i) \sum_j I_j^z(t)\cos(kz_j) \rangle}{\langle \sum_i I_i^z(0)\cos(kz_i) \sum_j I_j^z(0)\cos(kz_j) \rangle}. \tag{1.26}$$

The notation $c_{\mathcal{M}}(k,t)$ is used because Eq. (1.26) is the Fourier transform of the correlation function, $c_{ij}(t)$, as can be seen by expanding the cosines in Eq. (1.26) with the identity $\cos(a)\cos(b) = [\cos(a+b) + \cos(a-b)]/2$, and using translational invariance to eliminate the $\cos(a+b)$ term. The subscript $\mathcal{M}$ denotes magnetization, to differentiate this quantity from the energy correlation function to be introduced later. The magnetization operator is $\mathcal{M}_i \equiv \gamma\hbar I_i^z$. In terms its Fourier transform, $\mathcal{M}(k,t) = \sum_i \mathcal{M}_i(t)e^{ikz_i}$, we have $\sum_i \mathcal{M}_i(t)\cos(kz_i) = [\mathcal{M}(k,t) + \mathcal{M}(-k,t)]/2$. In-

serting this into Eq. (1.26), and using translational as well as time-reversal invariance, we find

$$c_{\mathcal{M}}(k,t) = \frac{\langle \mathcal{M}(-k,0)\mathcal{M}(k,t) \rangle}{\langle \mathcal{M}(-k,0)\mathcal{M}(k,0) \rangle}, \qquad (1.27)$$

It is observed experimentally that $c_{\mathcal{M}}(k,t) = \exp(-k^2 D_{\mathcal{M}} t)$, consistent with diffusive dynamics. $D_{\mathcal{M}}$ is the magnetization diffusion coefficient. In Refs. [2, 1], the results of many measurements with 1 μm $< k^{-1} <$ 3 μm and diffusion times between 10 and 60 s were fit to an exponential function, from which a diffusion coefficient was extracted. Their results are shown in Table 1.1.

1.3.2 Energy diffusion experiment

The measurement of energy diffusion requires two steps in addition to those discussed above for magnetization diffusion. The modulated z magnetization of Eq. (1.22) is first converted to a state with modulated energy density,

$$\sum_i I_i^z \cos(kz_i) \rightarrow \eta \sum_{i,j} \mathcal{H}_{ij} \frac{\cos(kz_i) + \cos(kz_j)}{2} + \text{higher order}, \qquad (1.28)$$

where $\mathcal{H}_{ij}$ is the pairwise dipolar interaction in front of the summation sign in Eq. (1.8) and $\eta < 1$ is the efficiency of the conversion. This is done using either of two NMR techniques. One is known as a Jeener-Broekaert (JB) pulse sequence,[16] and the other is called adiabatic demagnetization in the rotating frame (ADRF).[13] We do not discuss these techniques in detail, but refer the reader to the references already cited. The higher-order spin terms in Eq. (1.28) are not observed, so we neglect them from now on. The state, Eq. (1.28), evolves under the Hamiltonian, Eq. (1.8), for a time t, after which it becomes

$$\delta\rho(t) = \frac{1}{k_B TZ} \sum_{i<j;k<l} b_{ij} d_{ijkl}(t) \mathcal{H}_{kl} \cos(kz_i). \qquad (1.29)$$

Next, this state is converted back to observable z magnetization by the appropriate pulse sequence (a $\pi/4$ pulse if initialization was by JB, or an adiabatic remagnetization in the rotating frame if it was by ADRF). The gradient modulation is subsequently

27

unwound, yielding

$$\delta\rho(t+0) = \frac{1}{k_B T Z} \sum_{i<j;k<l} b_{ij} d_{ijkl}(t) \epsilon_{kl} \left[I_k^z \cos(kz_k) + I_l^z \cos(kz_l) \right] \cos(kz_i) \qquad (1.30)$$

where ϵ_{kl} is a dimensionless quantity proportional to b_{kl}. In the limit of infinitesimal polarization, the so-called dipolar ordered states of Eqs. (1.28) and (1.29) are local two-spin correlations. The length scale of these correlations (Å) is much smaller than the length scale of the spatial modulation (hundreds of nm), yielding $kz_i \approx kz_l$. As a consequence, the phase spread due to the creation and refocusing of dipolar order can also be safely ignored in the interpretation of these experiments. In the absence of transport, $kz_i \approx kz_k$, and the original state is recovered (scaled by 1/2, as before). As in the magnetization case, the residual phase term, $\cos k(z_i - z_k)$, encodes the spatial transport in the presence of spin diffusion. The final z magnetization is measured, as before, yielding

$$c_{\mathcal{H}}(k,t) = \frac{\langle \mathcal{H}(-k,0)\mathcal{H}(k,t) \rangle}{\langle \mathcal{H}(-k,0)\mathcal{H}(k,0) \rangle}, \qquad (1.31)$$

where we have defined $\mathcal{H}(k,t) \equiv \frac{1}{2} \sum_{i,j} [\mathcal{H}_{ij}(t) + \mathcal{H}_{ji}(t)] e^{ikz_i}$. Eq. (1.31) is the energy autocorrelation function in reciprocal space. It is found to be proportional to $\exp(-k^2 D_{\mathcal{H}} t)$, where the energy diffusion coefficient, $D_{\mathcal{H}}$, is different from the magnetization diffusion coefficient, $D_{\mathcal{M}}$. The results of many measurements with $1 \ \mu m < k^{-1} < 3 \ \mu m$ and diffusion times between 10 and 60 s are shown in Table 1.1.

1.4 Coherent vs incoherent transport

In the description above of the experiments on magnetization and energy diffusion in calcium fluoride, the details of the dynamics are contained in the correlation functions c_{ij} and d_{ijkl}. Evaluation of these terms for all t would entail solving a complicated many body problem. However, in order to compare the two diffusion processes and understand how the coherence of the dynamics may affect the results, it suffices to evaluate these correlation functions in the short time limit. The persistence of the

initial states is, to lowest order in t,

$$c_{ii}(t) = 1 - \frac{t^2}{4} \sum_k b_{ik}^2 + O(t^4). \tag{1.32}$$

$$d_{ijij}(t) = 1 - \frac{t^2}{4} \sum_k \left(b_{ik}^2 + b_{jk}^2 + b_{ik}b_{jk} \right) + O(t^4). \tag{1.33}$$

If the dipolar ordered state had been proportional to $I_i^z I_j^z$ only, then we would have $d_{ijkl} = c_{ik}c_{jl}$. The coefficient d in Eq. (1.33) differs from a simple product of the c's at this order by the cross terms $b_{ij}b_{jk}$. These types of cross terms vanish if one calculates the average diffusion coefficient for an equilibrium ensemble. (For example, they do not contribute to the moments of Eq. (1.31).) Because we cannot actually consider the system to be in equilibrium, in the sense of being coupled to a heat bath at a fixed temperature, this type of approach is questionable. One can easily imagine interference effects arising from a proliferation of cross terms such as the $b_{ik}b_{jk}$ of Eq. (1.33), though in this particular case they happen to be very small. (The sum of cross terms in Eq. (1.33) is an order of magnitude smaller than that of the other terms.) At present, there is no theory of such interference effects, if they exist. Nevertheless, both the smallness of the cross terms and the possibility to run the experiment several times to eliminate the effects of initial conditions, motivates us to pursue a statistical approach. Such an approach should be capable of capturing interference effects that are independent of the initial state, as discussed in the introductory paragraphs to this chapter.

1.5 Previous work

After Bloembergen introduced his phenomenological theory of relaxation by diffusion of nuclear spin magnetization to the sites of paramagnetic impurities, several authors performed microscopic calculations of this effect. These calculations fall broadly into two categories, the first being approaches based on quantum mechanics, the second being classical simulations. The former have historically required the use of various, sometimes crude, approximations. The latter, while being largely free of approx-

imations, say nothing about the quantum correlations in which we are interested. Nevertheless, some useful information has been obtained on the similarities between quantum and classical versions of spin diffusion.[17]

The first calculations were limited to magnetization transport. They were based on Bloembergen's diffusion equation, Eq. (1.12), which was extended to include the effects of paramagnetic impurities. This was done by Khutsishvili,[18] and also by DeGennes[19] and Redfield.[20] Building on these approaches Blumberg[21] showed that different regimes of magnetization diffusion are possible based on the concentration of impurites. For high impurity concentration the decay of non-equilibrium nuclear magnetization is dominated by direct relaxation of nuclei by impurity spins, while for low impurity concentration spin diffusion is important. The two cases have different experimental signatures and so can be distinguished. These predictions were verified experimentally by Blumberg and later by Goldman.[22] This convergence of theory and experiment put the phenomenon of spin diffusion on a firm foundation.

More sophisticated approaches geared towards a full quantum mechanical solution followed. A hydrodynamic calculation was given by Buishvili and Zubarev,[23] who studied the combined problem of nuclei coupled to rapidly relaxing impurities using non-equilibrium statistical mechanics. Integrodifferential equations for the spin autocorrelation functions of an isolated paramagnetic spin system were set up by Bennett and Martin,[24] who used a moment method for their solution. Their approach necessitated the uncontrolled approximation of the kernals of certain integrals by gaussians. An equation of motion approach was developed by Lowe and Gade,[25] and Kaplan,[26] who derived a diffusion equation for the expectation value of the magnetization in a state which was perturbed from equilibrium, and treated the flip-flop (or XY) term to first order in perturbation theory. Borckmans and Walgraef[27] used Prigogine's non-equilibrium statistical mechanics, and developed a diagrammatic technique to treat the flip-flop term to all orders, yet their approach also necessitated the replacement of certain integral kernels by gaussians in order to obtain a tractable solution. All of these methods gave reasonable agreement with each other, as well as with experiments measuring the diffusion coefficient of magnetization.

Energy, or heat transport, was not discussed until the later work of Redfield and Yu,[28] and Borckmans and Walgraef.[29] The relative neglect of this problem was presumably due to lack of experimental motivation, coupled with the increased difficulty of the calculations. The experimental motivation came with the measurements of magnetization[6] and energy[7] diffusion coefficients for the exchange-coupled nuclei of solid ^{3}He. Redfield and Yu obtained values for these coefficients based on Redfield's moment method. Although the ^{3}He experiments measured the energy diffusion rate to be roughly twice the spin diffusion rate, Redfield and Yu's calculation gave the same value for both. Although their ratio disagreed, their magnetization diffusion coefficient was accurate. Borckmans and Walgraef used their previous non-equilibrium approach to obtain energy diffusion coefficients for calcium fluoride that were slightly smaller than measured, but whose ratio was almost a factor of two, showing a more rapid diffusion of energy than magnetization. They also found the coefficients of both magnetization and energy diffusion to be roughly the same for solid ^{3}He, in agreement with Redfield and Yu but disagreeing with experiments.

The next significant development was that of computer simulations of classical spins.[30, 17] These simulations solved the Larmor precession equations of classical magnetic moments precessing in the fields from the surrounding spins as well as the external field. The simulations displayed diffusive behavior of both magnetization and energy, with energy diffusion being a factor of two faster than magnetization diffusion for dipolar coupled spins, but gave the same values for both coefficients in the case of exchange coupling, a result similar to that found by Redfield and Yu, and Borckmans and Walgraef. The diffusion coefficients for magnetization agreed with experiments, however.

Following this, Sodickson and Waugh[17] presented a proof, using spin coherent states, that a quantum mechanical analysis of magnetization diffusion reduces to the classical one in the limit of long-wavelength, high-temperature perturbations to the equilibrium state. This explained the agreement of quantum mechanical calculations with the computer simulations discussed above.

More recently, there has been a great deal of work on quantum spin chains, where

the question of the existence or absence of spin diffusion has been a controversy for many years. In this connection there have been experiments by Sologubenko et al.[12] that show diffusive behavior of both magnetization and energy in Haldane gapped, insulating spin-1 chains at high temperature, which show a striking resemblance to what is predicted by the theories described above. A theory of spin diffusion in such systems was developed by Sachdev and Damle.[31, 32] The situation in spin-1/2 chains is very different, where many authors have shown the ballistic, rather than diffusive, nature of excitations at high temperature.[33, 34, 35] We will not be concerned with the unique and sometimes surprising properties that are particular to lower-dimensional systems, but instead present a general analysis of the physics that is independent of dimension.

Chapter 2

Limit of large flip-flop term – XY model

In this chapter, we calculate the magnetization and energy (or thermal) diffusion coefficients at infinite temperature for the Hamiltonian, Eq. (1.1), in the limit $A_{ij} \to$ 0. This limit gives the XY model well-known in the study of magnetism. Since the B_{ij} term is responsible for the "flip-flop" process driving the dynamics of spin diffusion, our analysis is important for determining whether the Ising (A_{ij}) term can be neglected for spin diffusion in systems where $A_{ij} \neq 0$. To this end, we make a comparison to experimental data on calcium fluoride by taking $B_{ij} = -\frac{1}{2}b_{ij}$, with b_{ij} given by Eq. (1.2).

We use a moment method to obtain diffusion coefficients from the correlation functions, Eq. (1.27) and Eq. (1.31). This is a very direct, albeit phenomenological approach, and is well suited for the needs of this chapter. Unfortunately, this approach becomes extremely cumbersome when $A_{ij} \neq 0$. The calculation is simplified by a diagrammatic technique that is elaborated in Appendix A. We find the energy diffusion coefficient to be slightly larger than the magnetization diffusion coefficient for dipolar coupling, with the [001] orientation of the external field with respect to the crystal axes, giving qualitative agreement with experiments on calcium fluoride. The anisotropy of the magnetization diffusion coefficient is also in agreement, though its value is not. We attempt to obtain better agreement by taking the Ising (A_{ij})

term fully into account in the next chapter.

2.1   Moment method

The moment method for spin diffusion was introduced by DeGennes[19] and Redfield,[20] who in turn adapted it from Van Vleck's[15] method of determining the NMR line-shape. It is properly considered a phenomenological method rather than a microscopic one, since it introduces, by hand, an ad-hoc cutoff to frequency integrals in order to make them converge. This cutoff is in principle dependent on the microscopic dynamics of the model, but how to derive it from first principles is still an open problem. The form of the cutoff function is important as it plays a role in the magnitude of the diffusion coefficient calculated by the moment method. The situation is somewhat remedied if we ask for the ratio of the magnetization and energy diffusion coefficients (or, for a more general model with more conserved quantities, the ratio of any two diffusion coefficients). Assuming the cutoff function is of the same *form* in the two cases (with up to a single variable parameter), the ratio of diffusion coefficients is independent of the cutoff function. A gaussian cutoff therefore gives the same answer as a step function, for example.

In Chapter 1 we discussed experiments that measure the correlation function

$$c_S(k,t) = \frac{\langle S(-k,t)S(k,0)\rangle}{\langle S(-k,0)S(k,0)\rangle},\qquad(2.1)$$

where S stands for either magnetization, $S = \mathcal{M}$, or energy, $S = \mathcal{H}$, and the angular brackets denote averaging over the infinite temperature ensemble, $\langle\cdots\rangle = \mathrm{tr}\,\{\cdots\}/\,\mathrm{tr}\,\{1\}$. Expanding (2.1) in Taylor series about $t = 0$, we obtain

$$c_S(t) = \sum_{n=0}^{\infty} \frac{1}{(2n)!} M_S^{(2n)} t^{2n}.\qquad(2.2)$$

34

The even moments $M_S^{(2n)}$ are given by

$$M_S^{(2n)} = (-1)^n \left(\frac{1}{\hbar}\right)^{2n} \frac{\langle S(k,0)[\mathcal{H}, S(-k,0)]_{2n}\rangle}{\langle S(-k,0)S(k,0)\rangle}, \tag{2.3}$$

where $[A, B]_n \equiv [A, [A, [...[A, B]...]]]$, with A appearing n times. The sum in Eq. (2.2) involves only even powers of t because the odd moments are zero. These expressions may be derived by expanding $S(k, t) = e^{i\mathcal{H}t}S(k, 0)e^{-i\mathcal{H}t}$ by the well-known formula $e^A B e^{-A} = \sum_{n=0}^{\infty} \frac{1}{n!}[A, B]_n$ and putting the result in Eq. (2.1).

On timescales long compared with spin-spin dephasing but short compared with spin-lattice relaxation, Eq. (2.1) behaves as a solution to a diffusion equation. That is, experiments measure

$$c_S(t) = e^{-t/\tau_S}, \tag{2.4}$$

where $\tau_S = 1/(k^2 D_S)$, with k the wavenumber of the applied spatial modulation and D_S a constant diffusion rate that depends on the state $S = \mathcal{M}$ or $\mathcal{H}$. This expression has been shown to hold over a broad range of k and t.[2, ?] However, one immediately notices that, while (2.1) must be an even function of t, (2.4) is not. To reconcile these facts, we follow the argument of Redfield.[20]

First, let us write $c_S(t)$ in terms of its even Fourier transform.

$$c_S(t) = \int_0^\infty c_S(\omega) \cos \omega t \, d\omega. \tag{2.5}$$

Then the moments M_{2n} are given by expanding the cosine in Taylor series.

$$M_S^{(2n)} = (-1)^n \int_0^\infty \omega^{2n} c_S(\omega) d\omega \tag{2.6}$$

Now, the Fourier transform of e^{-t/τ_S} is a Lorentzian,

$$\int_0^\infty e^{-t/\tau_S} \cos(\omega t) \, dt = \frac{2\tau_S}{\pi} \frac{1}{1 + \omega^2 \tau_S^2}. \tag{2.7}$$

This function, however, has infinite moments. Therefore we make the assumption that $c_S(t) = e^{-t/\tau_S}$ for $t \gg T_S$, where $T_S \ll \tau_S$ is some timescale on the order of

35

the spin-spin dephasing time, but that for $t < T_S$ the behavior of $c_S(t)$ is unknown to us, except that it must be an even function around $t = 0$. One of the results of this chapter is a determination of this timescale in the case of dipolar-coupling.

An equivalent way to phrase the above condition is to say that the Fourier transform, $c_S(\omega)$, is the same as the Fourier transform of e^{-t/τ_S} for $\omega << T_S^{-1}$, but behaves differently for $\omega > T_S^{-1}$. In order for the odd time derivatives of $c_S(t)$ near $t = 0$ to be zero, and for the moments $M_S^{(2n)}$ to converge, we must have $c_S(\omega) \to 0$ for $\omega > T_S^{-1}$. We accomplish this by *assuming*

$$c_S(\omega) = \frac{2\tau_S}{\pi} \frac{1}{1 + \omega^2 \tau_S^2} g_S(\omega), \tag{2.8}$$

where we have introduced a frequency space cutoff function, $g_S(\omega) = 1$ for $\omega << T_S^{-1}$ and $g_S(\omega) \to 0$ for $\omega > T_S^{-1}$. Then, by equation (2.6),

$$\begin{aligned} M_S^{(2n)} &= (-1)^n \frac{2\tau_S}{\pi} \int_0^\infty \frac{\omega^{2n}}{1 + \omega^2 \tau_S^2} g_S(\omega) d\omega \\ &\simeq (-1)^n \frac{2}{\pi \tau_S} \int_0^\infty \omega^{2n-2} g_S(\omega) d\omega, \end{aligned} \tag{2.9}$$

for $n \geq 1$, while $M_S^{(0)} = 1$. Therefore,

$$M_S^{(2n)} = \frac{\alpha_{2n}}{T_S^{2n-1} \tau_S}, \tag{2.10}$$

with the coefficient of proportionality, α_{2n}, depending only on the shape of the cutoff function. Since $\tau_S = 1/(k^2 D_S)$, each moment calculated from Eq. (2.3) must have a leading k-dependence of k^2 in order for the theory to be self-consistent. In the next section will show that this is in fact the case.

Two reasonably simple possibilities for the cutoff function are a gaussian and a step function. These result in

$$\alpha_{2n} = \begin{cases} \frac{(-1)^n (2n-2)!}{\sqrt{\pi} 2^{2n-2} (n-1)!}, & g_S(\omega) = e^{-\omega^2 T_S^2} \\ \frac{(-1)^n 2}{\pi (2n-1)}, & g_S(\omega) = \Theta(T_S^{-1} - \omega) \end{cases} \tag{2.11}$$

36

Whatever the shape of the cutoff function, the diffusion coefficient can be expressed in terms of the second and fourth moments only, as

$$D_S = \frac{1}{k^2 \tau_S} = \frac{1}{k^2} \sqrt{\frac{\alpha_4}{\alpha_2^3} \frac{(M^{(2)})^3}{M^{(4)}}}. \tag{2.12}$$

Since each moment is proportional to k^2, this expression for D_S is independent of k. If we further assume that the functional form of $g_S(\omega)$ is independent of S, that is $g_S(\omega) = g(\omega, T_S)$, then the ratio of the two diffusion coefficients contains no free parameters, and we have

$$\frac{D_{\mathcal{H}}}{D_{\mathcal{M}}} = \sqrt{\frac{M_{\mathcal{M}}^{(4)}}{M_{\mathcal{H}}^{(4)}} \left(\frac{M_{\mathcal{H}}^{(2)}}{M_{\mathcal{M}}^{(2)}}\right)^3} \tag{2.13}$$

This assumption cannot be justified rigorously within this phenomenological theory, but it is believed to be reasonable.

2.2   Calculation of moments

In this section we calculate the second and fourth moments of magnetization and energy for the XY model, which is obtained from Eq. (1.1) by setting $A_{ij} = 0$,

$$\mathcal{H}_{XY} = \sum_{i,j} B_{ij} I_i^+ I_j^-. \tag{2.14}$$

Since we are interested in the long-wavelength behavior, we Taylor expand the correlation function, Eq. (2.1), in k. This gives

$$\begin{aligned}
c_S(k,t) &= \frac{\sum_{i,j} e^{ik(z_i - z_j)} \langle S_i(0) S_j(t) \rangle}{\sum_i \langle S_i(0)^2 \rangle} \\
&\simeq 1 - \frac{k^2}{2} \frac{\sum_{i,j} z_{ij}^2 \langle S_i(0) S_j(t) \rangle}{\sum_i \langle S_i(0)^2 \rangle} + O(k^4),
\end{aligned} \tag{2.15}$$

where $z_{ij} \equiv z_i - z_j$, and the terms odd in z_{ij} are zero. The $O(k^4)$ term is safely neglected as the correlation $\langle S_i(0) S_j(t) \rangle$ is a rapidly decaying function of the distance $|\mathbf{r}_i - \mathbf{r}_j|$. It depends on products of the inter-spin couplings, B_{ij}, which are either

short-ranged or, in the case of dipolar coupling, decay algebraically on a length scale of a few lattice spacings. We will demonstrate this explicitly for each moment. The wavelength, $\lambda = 2\pi/k$, is taken to be much longer than this decay scale. In the calcium fluoride experiments[2] it is at least 10^4 lattice spacings. Expanding the commutator in Eq. (2.3), we obtain

$$M_S^{(2n)} = \frac{(-1)^{n+1}k^2}{2\sum_i\langle S_i(0)^2\rangle}\sum_{i,j}z_{ij}^2\sum_{m=0}^{2n}\left(\begin{array}{c}2n\\m\end{array}\right)(-1)^m\langle \mathcal{H}^m S_j(0)\mathcal{H}^{2n-m}S_i(0)\rangle, \qquad (2.16)$$

for $n \geq 1$. Here $\left(\begin{array}{c}2n\\m\end{array}\right) = \frac{2n!}{m!(2n-m)!}$ is the binomial coefficient, and we have used

$$[\mathcal{H}, S_j(0)]_{2n} = \sum_{m=0}^{2n}\left(\begin{array}{c}2n\\m\end{array}\right)(-1)^m\mathcal{H}^m S_j(0)\mathcal{H}^{2n-m}. \qquad (2.17)$$

Eq. (2.16) proves the k^2 dependence mentioned in the last section.

To calculate the moments for the XY model from Eq. (2.16), one must evaluate averages of the form $\langle \mathcal{H}^m S_j(0)\mathcal{H}^{2n-m}S_i(0)\rangle$ for $\mathcal{H} = \mathcal{H}_{XY}$ and $S = \mathcal{M}$ or $\mathcal{H}$. This is most efficiently and elegantly done with the help of the diagrammatic technique introduced by Brout and co-workers.[36, 37, 38, 39] This technique eliminates the need for keeping track of the Kronecker deltas that arise from the contractions of spin operators, and allows the identification of the most important contributions to Eq. (2.16) at each n. For the case of infinite temperature that we are interested in, a tremendous simplification results because many of the ordered cumulants, which are introduced in Appendix A, vanish, thereby reducing the number of diagrams we need to consider. A detailed derivation of the technique is presented in Appendix A.

2.2.1 Magnetization moments

Consider the expression,

$$T_{2n} = (-1)^{n+1} \sum_{i,j} z_{ij}^2 \sum_{m=0}^{2n} \binom{2n}{m} (-1)^m \langle \mathcal{H}^m I_j^z \mathcal{H}^{2n-m} I_i^z \rangle, \qquad (2.18)$$

in the numerator of Eq. (2.16). We begin by associating a diagram element with each operator appearing in this expression, as follows.

$$I_i^z \longrightarrow \odot \qquad (2.19)$$

$$\mathcal{H} = \sum_{kl} B_{kl} I_k^+ I_l^- \longrightarrow l \qquad (2.20)$$

To the interaction is associated a directed line, with the arrow pointing away from the end corresponding to the I_k^+ operator and towards the end corresponding to the I_l^- operator. The indices k, l are dummies that are summed over, and in practice can be left off of diagrams.

Each diagram element receives a number based on the order in which it appears in the trace. This order must be kept track of because of the non-trivial commutation properties of spin operators. (This is in contrast to the diagrammatic technique for bosons or fermions, where Wick's theorem allows a factorization of operator averages, making the order unimportant. There is no analogue of Wick's theorem for averages of spin operators.) For example, the term $\langle I_i^z \mathcal{H} I_j^z \mathcal{H} \mathcal{H} \mathcal{H} \rangle$ has the diagrams numbered as follows.

Next, the diagram elements are joined end-to-end in all possible topologically distinct ways, with the circle diagrams, ∘, inserted at vertices. To each vertex is assigned an ordered cumulant, the order depending on the order of the diagram elements making

Figure 2-1: Diagram contributing to second moment for magnetization

up the vertex. The value of the diagram is found by taking the product of the ordered cumulants associated with it, multiplied by the factors associated with the interaction lines, and summing over all vertices without restriction (not including vertices with circles). The sum includes a factor of z_{ij}^2. One then sums the diagrams multiplied by the appropriate binomial coefficients appearing in Eq. (2.18). We note that the ordered cumulants are the analogues of the Green's functions appearing in field theoretic approaches to interacting fermion and boson problems. In the present approach, these quantities are associated with the vertices of the diagrams instead of with the lines. This is more natural because there can be any (even) number of lines connected to a vertex.

In constructing diagrams, the following rules hold. Not more than one circle diagram can occupy a given vertex, since the z_{ij}^2 factor in Eq. (2.18) ensures that $i \neq j$. There can be no free ends and no free circle diagrams, as these represent uncontracted spin operators which cause the trace to vanish. Each vertex must have the same number of lines leaving as entering, since the only non-zero ordered cumulants contain the same number of raising and lowering operators. Finally, the disconnected diagrams vanish, as shown in Appendix A.

We illustrate the above rules in the calculation of the second moment. The only diagram contributing to the second moment is shown in Fig. 2-1. Its contribution to Eq. (2.18) is

$$T_2 = \sum_{ij} z_{ij}^2 \sum_{m=0}^{2} \binom{2}{m} (-1)^m \times \begin{smallmatrix} 4 \\ \text{\raisebox{0.5ex}{\scriptsize diagram}} \\ m \end{smallmatrix}$$

$$\left[1 \times \left({}_2\!\!\bigcirc\!\!{}_3 + {}_3\!\!\bigcirc\!\!{}_2 \right) - 2 \times \left({}_1\!\!\bigcirc\!\!{}_3 + {}_3\!\!\bigcirc\!\!{}_1 \right) + 1 \times \left({}_2\!\!\bigcirc\!\!{}_1 + {}_1\!\!\bigcirc\!\!{}_2 \right) \right]$$

$$= \sum_{ij} z_{ij}^2 \times$$

$$= \sum_{ij} z_{ij}^2 B_{ij}^2 \left[\Big(\langle\langle z + - \rangle\rangle \langle\langle - + z \rangle\rangle + \langle\langle z - + \rangle\rangle \langle\langle + - z \rangle\rangle \Big) \right.$$

$$\left. - 2 \Big(\langle\langle + z - \rangle\rangle \langle\langle - + z \rangle\rangle + \langle\langle - z + \rangle\rangle \langle\langle + - z \rangle\rangle \Big) \right.$$

$$\left. + \Big(\langle\langle - + z \rangle\rangle \langle\langle + - z \rangle\rangle + \langle\langle + - z \rangle\rangle \langle\langle - + z \rangle\rangle \Big) \right]$$

$$= -\frac{1}{2} \sum_{ij} z_{ij}^2 B_{ij}^2. \tag{2.21}$$

The values of the ordered cumulants are $\langle\langle + - z \rangle\rangle = \frac{1}{4}$ and $\langle\langle - + z \rangle\rangle = -\frac{1}{4}$, and can be found in Table A.1.

The denominator of Eq. (2.16) is even simpler to calculate. No diagrams are necessary, and we obtain

$$\sum_i \langle (I_i^z)^2 \rangle = \frac{N}{4}. \tag{2.22}$$

Inserting these results into Eq. (2.16), we obtain

$$M_{\mathcal{M}}^{(2)} = -k^2 \sum_i z_{ik}^2 B_{ik}^2, \tag{2.23}$$

We note that, because of translational invariance, we can drop the summation over the dummy index k, since the analytic expressions there are independent of this index.

The diagrams contributing to the fourth moment for magnetization are shown in Fig. 2-2. They are calculated in a similar way to that just shown for the second moment, so we omit the details. Table A.1 shows that most of the fourth and fifth-order cumulants are zero, which enables us to consider only a subset of the orderings of the diagram elements. The non-zero cumulants at fourth and fifth order correspond to vertices with two ingoing and two outgoing lines, with both ingoing lines next to each other in the order (same for the outgoing lines). The calculation shows that only
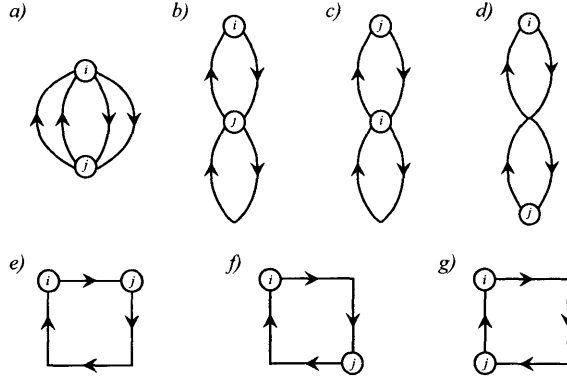
41

Figure 2-2: All topologically distinct diagrams containing two circles and four interaction lines. The diagrams shown here arise in the calculation of the fourth moment for magnetization as well as that of the second moment for energy. The analytic expressions for the diagrams are different in the two cases, however.

the diagrams labelled a), b), and c) in Fig. 2-2 contribute. The fourth moment is

$$M_{\mathcal{M}}^{(4)} = -4k^2 \left[\sum_i z_{ik}^2 B_{ik}^4 - \left(\sum_i z_{ik}^2 B_{ik}^2 \right) \left(\sum_i B_{ik}^2 \right) \right].$$

(2.24)

2.2.2 Energy moments

The expression in the numerator of Eq. (2.16) for energy, corresponding to Eq. (2.18), is

$$T_{2n} = (-1)^{n+1} \sum_{i,j,k,l} z_{ij}^2 \sum_{m=0}^{2n} \binom{2n}{m} (-1)^m \langle \mathcal{H}^m \mathcal{H}_{jl} \mathcal{H}^{2n-m} \mathcal{H}_{ik} \rangle.$$

(2.25)

We must symmetrize $\mathcal{H}_{ik}$ with respect to its indices. Letting

$$\mathcal{H}_{ik} = \mathcal{H}_{ik}^{(+)} + \mathcal{H}_{ik}^{(-)},$$

(2.26)

$$\mathcal{H}_{ik}^{(+)} \equiv \frac{1}{2} B_{ik} I_i^+ I_k^-,$$

(2.27)

$$\mathcal{H}_{ik}^{(-)} \equiv \frac{1}{2} B_{ik} I_i^- I_k^+,$$

(2.28)

we can rewrite Eq. (2.25) as

$$T_{2n} = 2 \left(T_{2n}^{(+)} + T_{2n}^{(-)} \right)$$

(2.29)

$$T_{2n}^{(+)} \equiv (-1)^{n+1} \sum_{i,j,k,l} z_{ij}^2 \sum_{m=0}^{2n} \binom{2n}{m} (-1)^m \langle \mathcal{H}^m \mathcal{H}_{jl}^{(+)} \mathcal{H}^{2n-m} \mathcal{H}_{ik}^{(+)} \rangle, \quad (2.30)$$

$$T_{2n}^{(-)} \equiv (-1)^{n+1} \sum_{i,j,k,l} z_{ij}^2 \sum_{m=0}^{2n} \binom{2n}{m} (-1)^m \langle \mathcal{H}^m \mathcal{H}_{jl}^{(+)} \mathcal{H}^{2n-m} \mathcal{H}_{ik}^{(-)} \rangle, \quad (2.31)$$

where use has been made of the formula

$$\langle (A + A^\dagger)(B + B^\dagger) \rangle = 2\mathrm{Re}\,\langle (A + A^\dagger)B \rangle, \quad (2.32)$$

for any operators A and B.

We associate the following diagram elements with the operators appearing in Eqs. (2.30) and (2.31).

$$\mathcal{H}_{ik}^{(+)} \longrightarrow \quad (2.33)$$

$$\mathcal{H}_{ik}^{(-)} \longrightarrow \quad (2.34)$$

The diagram element for the full interaction, $\mathcal{H}$, is the same as in the last section, i.e. Eq. (2.20). Dummy indices such as k will be left off of the diagrams as before.

The calculation of Eq. (2.25) is similar to that of Eq. (2.18). All possible topologically distinct, connected diagrams are formed from the elements in Eqs. (2.20), (2.33), and (2.34). The diagram corresponding to each term in Eq. (2.25) has its elements numbered based on the order in which they appear in the trace. Each vertex without a circle is assigned a dummy summation index, and each vertex with a circle receives the index corresponding to that circle. The circles corresponding to i and j must appear at different vertices. To each vertex is assigned an ordered cumulant according to the rules in Appendix A. Each interaction line has an interaction coefficient associated with it that has the appropriate indices. E.g. the line $k \longrightarrow l$ receives

43

a factor of B_{kl}. The interaction lines due to $\mathcal{H}_{ik}^{(+)}$ and $\mathcal{H}_{ik}^{(-)}$ receive an additional factor of $\frac{1}{2}$, because this factor appears in Eqs. (2.27) and (2.28). The analytical expression corresponding to a given diagram is formed by taking the product of all the ordered cumulants and interaction coefficients associated with it, and summing over all dummy indices without restriction. The result is multiplied by the factor 2 appearing in Eq. (2.29).

The diagrams contributing to the second moment for energy are shown in Fig. 2-2. These diagrams are exactly the same as the ones arising in the calculation of the fourth moment for magnetization. However, their meaning is different, as in this case there are no I^z operators, and we deal with a different set of ordered cumulants. We note that the diagrams at order (2n) for energy are always the same as those at order (2n+2) for magnetization.

One can easily see that the diagrams labelled $e)$, $f)$, and $g)$ in Fig. 2-2 are zero. Associated with each of them is the product of ordered cumulants, $\langle\langle +-\rangle\rangle^4 = \frac{1}{16}$. Because this cumulant factor is the same regardless of the order of diagram elements, we can move all the diagrams to the left of the second summation sign in Eq. (2.25). For example, diagram $e)$ gives

$$T_2(e) = 2\sum_{ij} z_{ij}^2 \sum_{m=0}^{2} \binom{2}{m} (-1)^m \times \begin{array}{c} \text{diagram} \end{array}$$

$$= 2\sum_{ij} z_{ij}^2 \times \begin{array}{c} \text{diagram} \end{array} \times \sum_{m=0}^{2} \binom{2}{m} (-1)^m. \qquad (2.35)$$

Since the sum over binomial coefficients is zero, we have $T_2(e) = 0$.

By direct calculation, it is also easily found that the diagrams labelled $a)$, $b)$, and $c)$ are zero. The only diagram contributing to the second moment for energy is therefore diagram $d)$ of Fig. 2-2. To illustrate the calculation procedure, we now evaluate this diagram.

44

Eq. (2.25) reads

$$T_2 = 2 \sum_{ij} z_{ij}^2 \sum_{m=0}^{2} \binom{2}{m} (-1)^m \times \left(\text{[diagram]} + \text{[diagram]} \right).$$

(2.36)

According to Table A.1, $\langle\langle + - + - \rangle\rangle = 0$. This restricts the possible orderings of the diagram elements, since not all vertices with four lines are allowed. Therefore,

$$T_2 = 2 \sum_{ij} z_{ij}^2 \times$$

$$\left| \left(\text{[diagram]} + \text{[diagram]} + \text{[diagram]} \right) \right.$$

$$- 2 \left(\text{[diagram]} + \text{[diagram]} \right)$$

$$+ \left. \left(\text{[diagram]} + \text{[diagram]} + \text{[diagram]} \right) \right|$$

(2.37)

The product of ordered cumulants is the same for each diagram in Eq. (2.37). It is $\langle\langle + - \rangle\rangle^2 \langle\langle + + - - \rangle\rangle = (\frac{1}{2})^2 (-\frac{1}{2}) = -\frac{1}{8}$. Multiplying by $\frac{1}{4}$ for the two circles, we

45

Figure 2-3: Diagram contributing to the denominator of Eq. (2.16) for energy.

obtain

$$T_2 = 2\left(-\frac{1}{8}\right)\left(\frac{1}{4}\right)\sum_{ijk} z_{ij}^2 B_{ik}^2 B_{jk}^2 \times [1(3) - 2(2) + 1(3)] = -\frac{1}{8}\sum_{ijk} z_{ij}^2 B_{ik}^2 B_{jk}^2. \quad (2.38)$$

The denominator of Eq. (2.16) is given by the diagram in Fig. 2-3. The corresponding analytic expression is $\langle\langle +-\rangle\rangle^2 \sum_{ij} B_{ij}^2 = \frac{1}{4}\sum_{ij} B_{ij}^2$. Inserting these results into Eq. (2.16), we obtain

$$M_{\mathcal{H}}^{(2)} = -\frac{k^2}{4}\frac{\sum_{ij} z_{ik}^2 B_{ij}^2 B_{jk}^2}{\sum_i B_{ik}^2}. \quad (2.39)$$

where we have used translational invariance to drop one of the summations.

The types of diagrams arising in the calculation of the fourth moment are shown in Fig. 2-4. To save space, the distinct topologies are pictured without circles. The entire set of diagrams at fourth order is obtained by placing two circles at the vertices of the diagrams in Fig. 2-4 in all possible ways. This set, along with the analytical expression associated with each diagram, is tabulated in Appendix B. Here we state the result.

$$\begin{aligned}
M_{\mathcal{H}}^{(4)} &= k^2 \sum_{ij} z_{ik}^2 B_{ik}^2 B_{jk}^2 - 2k^2\frac{\sum_{ij} z_{ik}^2\left(B_{ik}^2 B_{jk}^4 + B_{ik}^4 B_{jk}^2\right)}{\sum_i B_{ik}^2} - \frac{9}{4}k^2\frac{\sum_{ij} z_{ik}^2 B_{ik}^2 B_{jk}^2 B_{ij}^2}{\sum_i B_{ik}^2}\\
&\quad -\frac{k^2}{4}\frac{\sum_{ijl} z_{ik}^2\left(6B_{ik}^2 B_{jk}B_{kl}B_{ij}B_{il} - 18B_{ik}B_{jk}^2 B_{kl}B_{ij}B_{jl} + 11B_{jk}B_{kl}B_{ij}B_{il}B_{jl}^2\right)}{\sum_i B_{ik}^2}.
\end{aligned}$$

$$(2.40)$$

The sums over the index k are left off, as usual. The first term in Eq. (2.40) comes from diagrams a) and b). Diagram c) is of the same order of magnitude, and gives
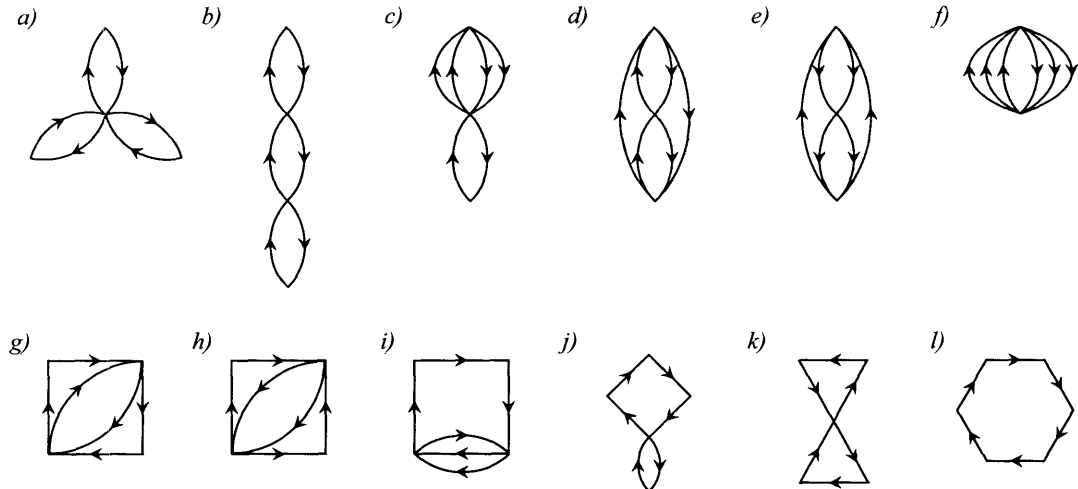
Figure 2-4: All topologically distinct diagrams containing six interaction lines. Diagrams for the fourth energy moment are obtained by placing circles with indices i and j at vertices in all distinct ways.

the second term in this equation. Diagrams $d)$ and $e)$ give rise to the third term, and are an order of magnitude smaller if the coupling is short-ranged, or even quasi-long ranged as in the case of dipolar coupled spins. Diagrams $g)$, $h)$, and $i)$ give the last term in Eq. (2.40) and are another order of magnitude smaller. The general guidelines are that those diagrams with either the highest power of the coupling constant or with the most factorizable summations over powers of coupling constants are the largest. The ones with several vertices joining only two lines, such as diagrams $g)$, $h)$, and $i)$, are the smallest. There are exceptions to these guidelines (For example, diagram $f)$ vanishes, for the same reason as does the corresponding diagram at second order.), but they are useful for allowing one to neglect those diagrams that are obviously small. As for the second moment, the diagrams $l)$ vanish, as do diagrams $j)$ and $k)$.

2.3   Numerical results for dipolar-coupled XY model

The results of numerical evaluation of the moments calculated in the last section for $B_{ij} = -\frac{1}{2}b_{ij}$, with b_{ij} given by Eq. (1.2), are given in Table 2.1. This corresponds to dipolar coupling. We have used values of the gyromagnetic ratio and lattice spacing

47

for the fluorines in calcium fluoride of $\gamma = 2.51 \times 10^4$ rad Hz/Oe and $a = 2.73 \times 10^{-8}$ cm. Because lattice sums can be evaluated numerically only for finite lattice sizes, we used finite size scaling to extract the infinite lattice limit. The approach to the infinite lattice value is expected to follow a power law. For example, if we approximate the sums by integrals in Eq. (2.23),

$$M_{\mathcal{M}}^{(2)} \approx -\frac{k^2}{4} \int_{a \leq r \leq L} d^3\mathbf{r}\, b(\mathbf{r})^2 z^2 \sim \text{const} \times \int_a^L r^2 dr \left(\frac{1}{r^3}\right)^2 r^2$$
$$= \text{const} \times \left(\frac{1}{a} - \frac{1}{L}\right). \qquad (2.41)$$

We performed a least squares fit to a power law of the quantities in Eqs. (2.23), (2.24), (2.39), and (2.40) as a function of lattice size, for both the [001] and [111] orientations of the crystal with respect to the external field. We found it sufficient to vary the lattice size between 1 and 81 lattice sites on an edge, in increments of 2 lattice sites. This gave agreement with Eq. (2.41) to better than one percent. The numbers in Table 2.1 are the infinite lattice values extracted from the scaling analysis.

Besides the moments, Table 2.1 gives the values for the diffusion coefficients for both gaussian and step-function cutoff, as well as the cutoff-independent ratio given by Eq. (2.13). We find fair agreement with experiments on calcium fluoride for the magnitudes of both diffusion coefficients. For magnetization, our value is slightly high, while for energy it is slightly low. The ratio $D_{\mathcal{H}}/D_{\mathcal{M}}$ that we calculate is about 1.6 for the [001] direction, while in these experiments it is between 4 and 5 (see Table 1.1). Given the phenomenological nature of the theory we feel this to be adequate agreement. For the [111] direction, the results are quite different, giving a ratio of diffusion coefficients that is less than one. We cannot account for this difference but conjecture that it may be the result of neglecting the Ising term from the calculation.

As an additional check for consistency of this theory we have calculated the value of the short time cutoff, T_S, from Eq. (2.10). As Table 2.1 shows, T_S was found to be on the order of 10 - 100 μs for the different cutoff functions and crystal orientations that we considered. This is consistent with our assumption of the relation of T_S to the spin-spin dephasing time given by the free induction decay. The timescale associated

48

Table 2.1: Summary of the results for the dipolar coupled XY model obtained from the moment method.

Moments	[001]	[111]	
$M_{\mathcal{M}}^{(2)}/k^2$ $(\times 10^{-7}\text{cm}^2/\text{s}^2)$	-5.59	-2.21	
$M_{\mathcal{M}}^{(4)}/k^2$ $(\times 10^3\text{cm}^2/\text{s}^4)$	1.56	0.130	
$M_{\mathcal{H}}^{(2)}/k^2$ $(\times 10^{-7}\text{cm}^2/\text{s}^2)$	-2.80	-1.08	
$M_{\mathcal{H}}^{(4)}/k^2$ (cm^2/s^4)	76.2	28.4	
Results for gaussian cutoff	[001]	[111]	D_{001}/D_{111}
$D_{\mathcal{M}}$ $(\times 10^{-12}\text{cm}^2/\text{s})$	13.3	11.4	1.17
$D_{\mathcal{H}}$ $(\times 10^{-12}\text{cm}^2/\text{s})$	21.2	8.4	2.5
$T_{\mathcal{M}}$ $(\times 10^{-6}\text{ s})$	13.4	35.8	
$T_{\mathcal{H}}$ $(\times 10^{-6}\text{ s})$	42.8	43.8	
Cutoff independent result			
$D_{\mathcal{H}}/D_{\mathcal{M}}$	1.59	0.74	

with this decay in calcium fluoride is approximately 20 μs with the external field in the [001] direction and approximately 50 μs with the external field in the [111] direction.[40]

2.4 Summary

The magnetization and energy diffusion coefficients for the XY model at infinite temperature have been calculated using a moment method. In the case of dipolar coupling, we found qualitative agreement with experiments on calcium fluoride for both diffusion coefficients. The ratio of the diffusion coefficient for energy to that for magnetization was found to be greater than one for the [001] orientation of the external field with respect to the crystal axes. However, this is not large enough to fully account for the observations. The orientation dependence of the diffusion coefficients was also in qualitative agreement for magnetization, but not for energy. The lack of any experimentally observed orientation dependence for energy diffusion leads us to conjecture that some other k-dependent decay processes may have been at play in the experiment, increasing the decay rate. To determine whether our approximation of dropping the Ising $(I^z I^z)$ term was too drastic, we fully retain this

term in the analysis of the next chapter.

Chapter 3

Hydrodynamics and perturbative treatment of flip-flop term

To obtain a theory for spin diffusion, one can try to proceed in either of two ways. One is to derive from first principles an equation for the average magnetization or energy density and to show that it is a diffusion equation, with a diffusion coefficient expressed in terms of microscopic quantities (the dipolar coupling constants). This type of approach is used in refs.[23, 41, 42, 25, 26]. Another approach is to *assume* that small amplitude, long-wavelength perturbations of magnetization or interaction energy relax to equilibrium through diffusion. This assumption is motivated by the conservation of the total energy and magnetization, as we shall see below, as well as by general physical principles, and by experiment. Given this assumption, a relationship may be derived between the diffusion coefficient and microscopic quantities. This relationship is then used to evaluate the diffusion coefficient.[43] We take the second type of approach, although there is also a way to obtain the same results by the first type of approach, as we discuss below.

This chapter is organized as follows. In sections 3.1 - 3.3 we outline the linear response formalism for spin diffusion in a solid, including a new derivation of the energy and magnetization current operators. This formalism applies to the high-temperature, long-wavelength regime studied experimentally. It is equivalent to the density matrix approach of Lowe and Gade,[25] and Kaplan[26] (LGK), as we prove

in section 3.2. Our formulation has the advantages that the long-wavelength limit is built-in and the application to inter-spin energy is straightforward. In section 3.4, we derive the expansion of the Kubo formula in powers of the flip-flop term of the Hamiltonian, which we use for numerical evaluation of the diffusion coefficients. The diffusion coefficients of magnetization and inter-spin energy obtained from this expansion to two leading orders in the flip-flop are given in section 3.5. Their numerical values are calculated in section 3.6, along with an estimate of the errors. Our main finding is that, although the expansion for the magnetization diffusion coefficient reproduces the experimental results quantitatively, the series for inter-spin energy produces only qualitative agreement. This is nevertheless a vast improvement over the results of Chapter 2. In section 3.7 we discuss this result and comment on how the methods presented in this chapter complement other approaches to the problem.

3.1 Hydrodynamic approach

We are interested in studying the effects of long-wavelength, small amplitude perturbations to the high-temperature equilibrium state, of globally conserved quantities. In a system of spins with Hamiltonian, Eq. (1.1), the total energy and magnetization along the external field are constant in time, and therefore local densities of these quantities must change in time in such a way that this constraint is satisfied. This is expressed mathematically as a continuity equation relating the density and current operators of the conserved quantities, in the Heisenberg representation, as

$$\frac{\partial \hat{S}(\mathbf{r}, t)}{\partial t} + \nabla \cdot \hat{\mathbf{j}}^{(S)}(\mathbf{r}, t) = 0, \tag{3.1}$$

where $S(\mathbf{r})$ is the operator representing the local density of a globally conserved quantity. In our case this is either the energy ($S = \mathcal{H}$) or the component of spin magnetization along an external field ($S = \mathcal{M}$), and $\mathbf{j}(\mathbf{r})$ is the corresponding current density. We derive Eq. (3.1) below for both cases. The discrete version of this formula is more directly applicable to our problem since the spins reside on a lattice,

52

and is given by replacing $\mathbf{r}$ with a lattice site index. However, the continuum representation is more useful for derivations, and is completely equivalent. A useful way of going between these two representations is to write the densities of magnetization and interaction energy in terms of the lattice variables as follows.[23, 42]

$$I^\alpha(\mathbf{r}, t) \equiv \sum_i \delta(\mathbf{r} - \mathbf{r}_i) I_i^\alpha(t), \quad \alpha = z, +, - \tag{3.2}$$

$$\mathcal{H}(\mathbf{r}, t) \equiv \sum_{i,j(i\neq j)} \delta(\mathbf{r} - \mathbf{r}_i) \mathcal{H}_{ij}(t). \tag{3.3}$$

These densities are then given in terms of the spin densities as

$$M(\mathbf{r}) = \gamma \hbar I_i^z(\mathbf{r}), \tag{3.4}$$

$$\mathcal{H}(\mathbf{r}) = \int d^3 \mathbf{r}' \left[A(\mathbf{r} - \mathbf{r}') I^z(\mathbf{r}) I^z(\mathbf{r}') + B(\mathbf{r} - \mathbf{r}') I^+(\mathbf{r}) I^-(\mathbf{r}') \right], \tag{3.5}$$

where we have used Eq. (1.1) for the Hamiltonian, and assumed the interactions depend only on the vector displacement between the spins. Explicitly, $A(\mathbf{r} - \mathbf{r}') = \sum_{i,j} \delta(\mathbf{r} - \mathbf{r}_i) \delta(\mathbf{r}' - \mathbf{r}_j) A_{ij}$, with a similar equation for $B(\mathbf{r} - \mathbf{r}')$.

Eq. (3.1) is as far as we can go on general grounds. In the first type of approach to a theory of spin diffusion mentioned in the introduction, we would try to derive a constitutive relation,

$$\langle \hat{\mathbf{j}}_S(\mathbf{r}, t) \rangle_{non-eq} = -D \nabla \langle \hat{S}(\mathbf{r}, t) \rangle_{non-eq}, \tag{3.6}$$

where $\langle \cdots \rangle_{non-eq}$ denotes a non-equilibrium average taken, for example, over one of the spatially varying states discussed in Chapter 1. This constitutive relation, when combined with Eq. (3.1), would give a diffusion equation for $\langle \hat{S}(\mathbf{r}, t) \rangle_{non-eq}$,

$$\left(\frac{\partial}{\partial t} - D \nabla^2 \right) \langle \hat{S}(\mathbf{r}, t) \rangle_{non-eq} = 0. \tag{3.7}$$

We do not use this approach, but instead assume Eq. (3.6) is true. This assumption is physically motivated. If we suppose the average current to depend on the magnetization and its gradients, and expand it in powers of these variables (since

we are interested in very small magnetization, such an expansion is reasonable) the lowest order term is that containing the gradient of magnetization. The coefficient of the term linear in magnetization is zero because no current flows in a spatially uniform state. But perhaps the best motivation is from experiment.

Having thus accepted Eq. (3.6), we will use some formal manipulations to obtain an expression for the diffusion coefficient in terms of the Kubo formula that is well-known from linear response theory. In the process, we will prove that using this formula is equivalent to calculating the diffusion coefficient by an equation of motion approach introduced by Lowe and Gade,[25] and Kaplan[26] (LGK).

3.2 Equation of motion method and the Kubo formula

Experimentally, spin diffusion has been measured by observing the relaxation of initial states varying sinusoidally in real space with a given wavevector $\mathbf{k}$.[2, 1] Such spatially-inhomogeneous states are represented mathematically as perturbations on the infinite temperature equilibrium state, $\rho_\infty = 1/2^N$, where N is the number of spins. We have

$$\rho(0) = \rho_\infty + \delta\rho(0). \tag{3.8}$$

Two possibilities exist for $\delta\rho(0)$, corresponding to long-wavelength fluctuations in the two conserved quantities,

$$\delta\rho_M(\mathbf{k}, 0) = \epsilon \int d^3\mathbf{r} \cos(\mathbf{k} \cdot \mathbf{r}) M(\mathbf{r}), \tag{3.9}$$

$$\delta\rho_\mathcal{H}(\mathbf{k}, 0) = \epsilon \int d^3\mathbf{r} \cos(\mathbf{k} \cdot \mathbf{r}) \mathcal{H}(\mathbf{r}), \tag{3.10}$$

where ϵ is a small quantity of order $\gamma\hbar B_0/2^N k_B T$. Here B_0 is the external field, and γ is the gyromagnetic ratio of the nuclear species of interest ($\gamma = 2.51 \times 10^4$ rad Hz/Oe for ^{19}F). The important length scales are related by $L \gg k^{-1} \gg a$, where L is the sample size and a is the lattice spacing. Typical values for these quantities in

the experiments were $L \sim 0.1\,\text{cm}$ and $k^{-1} \sim 10^{-4}\,\text{cm}$. $a = 2.73 \times 10^{-8}\,\text{cm}$ for the Fluorines in calcium fluoride. The experimental realization of such states has been discussed in detail in Chapter 1, as well as by Boutis et al.[1] In practice, $\mathbf{k}$ is parallel to the external magnetic field, and transport is measured in the same direction. As we saw in Chapter 1, expectation values taken with respect to the states in Eqs. (3.9) and (3.10) give rise to equilibrium-averaged correlation functions.

LGK compute the time evolution of the average density, $\langle S(\mathbf{k},t) \rangle = \text{tr}\{\delta\rho(-\mathbf{k},t)S(\mathbf{k})\}$, starting from one of the non-equilibrium states, Eq. (3.9) or Eq. (3.10). In general, we write

$$\delta\rho(t=0) = \epsilon \int d^3\mathbf{r} \cos(\mathbf{k}\cdot\mathbf{r})S(\mathbf{r}) = \frac{\epsilon}{2}S(\mathbf{k}) + \frac{\epsilon}{2}S(-\mathbf{k}). \qquad (3.11)$$

The average of any Schrödinger operator A at time t is

$$\langle A(t) \rangle = \text{tr}\{\delta\rho(t)A\}. \qquad (3.12)$$

If $\langle S(\mathbf{r},t) \rangle$ satisfies a diffusion equation,

$$\frac{\partial}{\partial t}\langle S(\mathbf{r},t)\rangle = D\nabla^2 \langle S(\mathbf{r},t)\rangle, \qquad (3.13)$$

then the time dependence of $\langle S(\mathbf{k},t)\rangle$ (the Fourier transform of $\langle S(\mathbf{r},t)\rangle$ at wavevector $\mathbf{k}$) is given by

$$
\begin{aligned}
\frac{\partial}{\partial t}\langle S(\mathbf{k},t)\rangle &= -Dk^2\langle S(\mathbf{k},t)\rangle \\
\implies \quad \langle S(\mathbf{k},t)\rangle &= e^{-k^2 D t}\langle S(\mathbf{k},0)\rangle.
\end{aligned}
\qquad (3.14)
$$

Taking the time derivative of the last equation and rearranging terms, we obtain LGK's expression for the diffusion coefficient,

$$D = \lim_{k\to 0}\left(-\frac{1}{k^2}\right)\frac{\langle \dot{S}(\mathbf{k},t)\rangle}{\langle S(\mathbf{k},0)\rangle}. \qquad (3.15)$$

The right hand side is in fact independent of time for t greater than the short timescale defined by the inverse spin-spin coupling. LGK showed this explicitly for magnetiza-

55

tion. We keep the explicit time dependence to remind us that t is long, but finite, while k tends to zero. In other words, we take the $t \to \infty$ limit after the $k \to 0$ limit.

In the Heisenberg representation, we have

$$
\begin{aligned}
\langle S(\mathbf{k}, t) \rangle = & \quad \text{tr} \left\{ e^{-i\mathcal{H}t} \delta\rho(0) e^{i\mathcal{H}t} S(\mathbf{k}) \right\} \\
= & \quad \frac{\epsilon}{2} \text{tr} \left\{ S(\mathbf{k}, -t) S(\mathbf{k}, 0) \right\} \\
& + \frac{\epsilon}{2} \text{tr} \left\{ S(-\mathbf{k}, -t) S(\mathbf{k}, 0) \right\}.
\end{aligned}
\tag{3.16}
$$

Because of translational invariance, only the second term on the right side of Eq. (3.16) contributes, and we have

$$
\langle S(\mathbf{k}, t) \rangle = \frac{\epsilon}{2} \text{tr} \left\{ S(-\mathbf{k}, -t) S(\mathbf{k}, 0) \right\}.
\tag{3.17}
$$

We take the time derivative of Eq. (3.17), and use $\partial S(t)/\partial t = i[\mathcal{H}, S(t)]$, to find

$$
\begin{aligned}
\langle \dot{S}(\mathbf{k}, t) \rangle = & \quad -i \frac{\epsilon}{2} \text{tr} \left\{ e^{-i\mathcal{H}t} [\mathcal{H}, S(-\mathbf{k}, 0)] e^{i\mathcal{H}t} S(\mathbf{k}, 0) \right\} \\
= & \quad -\frac{\epsilon}{2} \text{tr} \left\{ \dot{S}(-\mathbf{k}, 0) S(\mathbf{k}, t) \right\} \\
= & \quad -\frac{\epsilon}{2} \int_0^t dt' \, \text{tr} \left\{ \dot{S}(-\mathbf{k}, 0) \dot{S}(\mathbf{k}, t') \right\} \\
& - \frac{\epsilon}{2} \text{tr} \left\{ \dot{S}(-\mathbf{k}, 0) S(\mathbf{k}, 0) \right\}.
\end{aligned}
\tag{3.18}
$$

The second term on the right-hand side of the last equation vanishes. Substituting the continuity equation, $\dot{S}(\mathbf{k}, t) + i\mathbf{k} \cdot \mathbf{j}(\mathbf{k}, t) = 0$, and taking $\mathbf{k} = k\hat{z}$, we obtain

$$
\langle \dot{S}(\mathbf{k}, t) \rangle = -\frac{\epsilon}{2} k^2 \int_0^t dt' \, \text{tr} \left\{ j_z(\mathbf{k}, t') j_z(-\mathbf{k}, 0) \right\},
\tag{3.19}
$$

where j_z is the current density in the transport direction. According to Eq. (3.16), we further have

$$
\langle S(\mathbf{k}, 0) \rangle = \frac{\epsilon}{2} \text{tr} \left\{ S(\mathbf{k}, 0) S(-\mathbf{k}, 0) \right\}.
\tag{3.20}
$$

56

Substituting Eqs. (3.19) - (3.20) into Eq. (3.15) gives

$$D = \lim_{k \to 0} \frac{\int_0^t dt' \, \text{tr} \left\{ j_z(\mathbf{k}, t') j_z(-\mathbf{k}, 0) \right\}}{\text{tr} \left\{ S(\mathbf{k}, 0) S(-\mathbf{k}, 0) \right\}}. \qquad (3.21)$$

Taking the limit $t \to \infty$, and replacing the traces with infinite temperature equilibrium averages, $\text{tr} \left\{ \cdots \right\} = \text{tr} \left\{ \mathbf{1} \right\} \langle \cdots \rangle$, we obtain the standard form of the Kubo formula,[43]

$$D = \frac{\int_0^\infty dt \int d^3\mathbf{r} \int d^3\mathbf{r}' \langle j_z(\mathbf{r}, t) j_z(\mathbf{r}', 0) \rangle}{\int d^3\mathbf{r} \int d^3\mathbf{r}' \langle S(\mathbf{r}, 0) S(\mathbf{r}', 0) \rangle}. \qquad (3.22)$$

This proves the equivalence of LGK's approach and linear response theory.

Eq. (3.22) is the correct formula for the diffusion coefficient of the quantity S if the following assumptions hold.

(1) The correlation function of S is known to have a diffusive form (i.e. a diffusive pole).

(2) The system may at all times be described by a statistical ensemble that is sufficiently close to equilibrium (linear response regime).

Assumption (1) may be checked experimentally, and has been verified for both spin-spin and energy-energy correlators of dipolar-coupled spins in a solid.[2, 1] Assumption (2) is more subtle, as it rests on the validity of the ergodic hypothesis, which has received much attention recently in the context of lattice spin systems in dimensions 1 – 3.[44, 45, 46, 47, 48] This hypothesis states essentially what we discussed in Chapter 1, namely that we can consider the evolution of the system to be independent of its initial state, which is true if the experiment is performed many times and the results are averaged.

Regardless of the averaging obtained by many repetitions of the experiment, we also find it plausible that assumption (2) is valid when the spatial profile of magnetization or energy in the initial state varies sufficiently slowly, and when this state has no long range correlations. While this is possible for magnetization, the creation of spatial inhomogeneities in the interaction energy requires NMR techniques that introduce short - ranged correlations between the spins. Some of these correlations

persist due to energy conservation, and these are the ones relevant to energy transport. Other correlations are assumed to decay rapidly and to be unobservable. A careful analysis of the initial state involved in the energy diffusion measurements is needed to determine whether assumption (2) is satisfied.

3.3   Current Operators

In order to use Eq. (3.22) we need to obtain expressions for the current operators $j_z(\mathbf{r})$. We start with the Hamiltonian, Eq. (3.5), which conserves the total z-component of magnetization as well as the total energy. This suggests that the magnetization and energy densities each satisfy a local continuity equation.[43] These may be derived from the Heisenberg equation of motion,

$$\frac{\partial M(\mathbf{r},t)}{\partial t} = -\frac{i}{\hbar}[M(\mathbf{r},t),\mathcal{H}], \tag{3.23}$$

$$\frac{\partial \mathcal{H}(\mathbf{r},t)}{\partial t} = -\frac{i}{\hbar}[\mathcal{H}(\mathbf{r},t),\mathcal{H}], \tag{3.24}$$

which gives

$$\frac{\partial M(\mathbf{r})}{\partial t} = \frac{i\gamma\hbar}{2}\int d^3\mathbf{r}'b(\mathbf{r}-\mathbf{r}')\left(I_+(\mathbf{r})I_-(\mathbf{r}')-I_+(\mathbf{r}')I_-(\mathbf{r})\right),$$

$$\tag{3.25}$$

$$\frac{\partial \mathcal{H}(\mathbf{r})}{\partial t} = \frac{i}{4}\int d^3\mathbf{r}'d^3\mathbf{r}''b(\mathbf{r}'-\mathbf{r})b(\mathbf{r}''-\mathbf{r}')$$

$$\times\{I_z(\mathbf{r}')\left(I_+(\mathbf{r})I_-(\mathbf{r}'')-I_+(\mathbf{r}'')I_-(\mathbf{r})\right)$$

$$+2I_z(\mathbf{r})\left(I_+(\mathbf{r}')I_-(\mathbf{r}'')-I_+(\mathbf{r}'')I_-(\mathbf{r}')\right)$$

$$+2I_z(\mathbf{r}'')\left(I_+(\mathbf{r})I_-(\mathbf{r}')-I_+(\mathbf{r}')I_-(\mathbf{r})\right)\}. \tag{3.26}$$

In order to write Eqs. (3.25)-(3.26) as continuity equations in the usual form, they may be integrated over an arbitrary volume and the result expressed in terms of a surface integral, whose integrand is the current density. For example, integrating

Eq.(3.25) over a spherical volume V gives

$$\int_V d^3\mathbf{r}\frac{\partial \mathcal{M}(\mathbf{r})}{\partial t} = \frac{i\gamma\hbar}{2}\int_V d^3\mathbf{r}\int d^3\mathbf{r}'b(\mathbf{r}'-\mathbf{r})(I_+(\mathbf{r})I_-(\mathbf{r}')-I_+(\mathbf{r}')I_-(\mathbf{r})). \qquad (3.27)$$

Changing variables to $\mathbf{y} = \mathbf{r} - \mathbf{r}'$, we obtain

$$\int_V d^3\mathbf{r}\frac{\partial \mathcal{M}(\mathbf{r})}{\partial t} = \frac{i\gamma\hbar}{2}\int d^3\mathbf{y}b(\mathbf{y})\int_V d^3\mathbf{r}[I_+(\mathbf{r})I_-(\mathbf{r}-\mathbf{y})-I_+(\mathbf{r}-\mathbf{y})I_-(\mathbf{r})]. \qquad (3.28)$$

Changing now the limits of integration, this becomes

$$\int_V d^3\mathbf{r}\frac{\partial \mathcal{M}(\mathbf{r})}{\partial t} = \frac{i\gamma\hbar}{2}\int d^3\mathbf{y}b(\mathbf{y})\int_{V-\mathbf{y}} d^3\mathbf{r}[I_+(\mathbf{r}+\mathbf{y})I_-(\mathbf{r})-I_+(\mathbf{r})I_-(\mathbf{r}+\mathbf{y})]. \qquad (3.29)$$

Taylor expanding the second integral about the original limit, using $\int_{V-\mathbf{y}} d^3\mathbf{r} \approx \int_V d^3\mathbf{r} - \mathbf{y}\cdot\oint_V d\mathbf{S}$, gives

$$
\begin{aligned}
\int_V d^3\mathbf{r}\frac{\partial \mathcal{M}(\mathbf{r})}{\partial t} &= \frac{i\gamma\hbar}{4}\int d^3\mathbf{y}b(\mathbf{y})\mathbf{y}\cdot\int_{S_V} d\mathbf{S}[I_+(\mathbf{r})I_-(\mathbf{r}+\mathbf{y})-I_+(\mathbf{r}+\mathbf{y})I_-(\mathbf{r})]\\
&= \int_{S_V} d\mathbf{S}\cdot\mathbf{j}^{(\mathcal{M})}(\mathbf{r},t), \qquad (3.30)
\end{aligned}
$$

A similar, but longer derivation gives the energy current. In this manner we obtain the current density operators,

$$
\begin{aligned}
\mathbf{j}^{(\mathcal{M})}(\mathbf{r},t) = \quad &\frac{i\gamma\hbar}{4}\int d^3\mathbf{r}'b(\mathbf{r}-\mathbf{r}')(\mathbf{r}-\mathbf{r}')\\
&\times (I_+(\mathbf{r})I_-(\mathbf{r}')-I_+(\mathbf{r}')I_-(\mathbf{r})), \qquad (3.31)\\
\mathbf{j}^{(\mathcal{H})}(\mathbf{r},t) = \quad &\frac{i}{8}\int d^3\mathbf{r}'d^3\mathbf{r}''b(\mathbf{r}'-\mathbf{r})b(\mathbf{r}''-\mathbf{r}')(\mathbf{r}-\mathbf{r}'')\\
&\times\{I_z(\mathbf{r}')\left(I_+(\mathbf{r})I_-(\mathbf{r}'')-I_+(\mathbf{r}'')I_-(\mathbf{r})\right)\\
&+2I_z(\mathbf{r})\left(I_+(\mathbf{r}')I_-(\mathbf{r}'')-I_+(\mathbf{r}'')I_-(\mathbf{r}')\right)\\
&+2I_z(\mathbf{r}'')\left(I_+(\mathbf{r})I_-(\mathbf{r}')-I_+(\mathbf{r}')I_-(\mathbf{r})\right)\}, \qquad (3.32)
\end{aligned}
$$

The continuity equations then take the usual form of Eq. (3.1). Similar results have been obtained by Furman and Goren by a different method.[42, 49]

3.4 Perturbation Theory

Using an interaction representation introduced by Lowe and Norberg,[40] we can expand Eq. (3.22) in powers of the flip-flop term of the Hamiltonian. Following Ref. [25] we define

$$\mathcal{H}_1 = \sum_{i,j(i\neq j)} A_{ij}\, I_{iz}I_{jz}, \qquad (3.33)$$

$$\mathcal{H}_2 = \sum_{i,j(i\neq j)} B_{ij}\, I_{i+}I_{j-}. \qquad (3.34)$$

Using the notation $\tilde{A}(t) = e^{-i\mathcal{H}_1 t/\hbar} A(0) e^{i\mathcal{H}_1 t/\hbar}$, we may write any operator in the Heisenberg representation as an infinite series in $\mathcal{H}_2$,

$$\begin{aligned}
A(t) \;=\; e^{i\mathcal{H}_1 t/\hbar} &\left\{ A(0) + \frac{i}{\hbar}\int_0^t dt_1\, [\tilde{\mathcal{H}}_2(t_1), A(0)] \right. \\
&\left. + \left(\frac{i}{\hbar}\right)^2 \int_0^t dt_1 \int_0^{t_1} dt_2\, [\tilde{\mathcal{H}}_2(t_1), [\tilde{\mathcal{H}}_2(t_2), A(0)]] + \cdots \right\} e^{-i\mathcal{H}_1 t/\hbar}. \quad (3.35)
\end{aligned}$$

Using this expansion for $j_z(t)$ in Eq. (3.22) gives a perturbation series for the diffusion coefficient.

$$\begin{aligned}
D \;=\; \frac{1}{\langle S(0)^2\rangle} &\left(\int_0^\infty dt\, \mathrm{tr}\,\{j_z(0)\tilde{j}_z(t)\} + \frac{i}{\hbar}\int_0^\infty dt \int_0^t dt_1\, \mathrm{tr}\,\{[\tilde{\mathcal{H}}_2(t_1), j_z(0)]\tilde{j}_z(t)\} \right. \\
&\left. + \left(\frac{i}{\hbar}\right)^2 \int_0^\infty dt \int_0^t dt_1 \int_0^{t_1} dt_2\, \mathrm{tr}\,\{[\tilde{\mathcal{H}}_2(t_1), [\tilde{\mathcal{H}}_2(t_2), j_z(0)]] \times \tilde{j}_z(t)\} + \cdots \right),
\end{aligned}$$

$$(3.36)$$

where the spatial integrations have been suppressed. The operators $\tilde{\mathcal{H}}_2(t)$ and $\tilde{j}_z(t)$ can be evaluated using the identity,[40, 25]

$$\begin{aligned}
\exp &\left(it \sum_{m,n(m\neq n)} A_{mn} I_{mz} I_{nz} \right) I_{i+} I_{j-} \\
&\times \exp\left(-it \sum_{m,n(m\neq n)} A_{mn} I_{mz} I_{nz} \right) = I_{i+} I_{j-} L_{ij}(t),
\end{aligned} \qquad (3.37)$$

60

where

$$L_{ij}(t) \equiv \prod_{l(l \neq i,j)} e^{2it(A_{li} - A_{lj})I_{lz}}.$$ (3.38)

It is advantageous to approximate the operator $L_{ij}(t)$ by a c-number, equal to its infinite-temperature thermal average, $L_{ij}(t) \approx G_{ij}(t)$, where

$$G_{ij}(t) = \prod_{m(m \neq i,j)} \cos(A_{im} - A_{jm})t.$$ (3.39)

The neglected q-number terms are expected to be approximately $20 - 25\%$ smaller, as discussed at the end of section 3.5.

It turns out that $G_{ij}(t)$ depends very weakly on its indices. In order to make the calculation of higher order terms in the perturbation series tractable, we therefore replace $G_{ij}(t)$ by $G(t)$. G is a suitably defined average over all the G_{ij}'s, as discussed in section 3.6. The overall error introduced by approximating the higher order terms in this way is therefore small (we shall see in section 3.6 that it is less than 10%). The resulting perturbation series contains only even-order terms,

$$D = \sum_{n=0}^{\infty} \left(\frac{1}{\hbar}\right)^{2n} \frac{F^{2n+1}}{(2n+1)!} \frac{\langle [\mathcal{H}_2, j_z(0)]_n^2 \rangle}{\langle S(0)^2 \rangle},$$ (3.40)

$$F \equiv \int_0^{\infty} G(t)\, dt,$$ (3.41)

where $[A, B]_n \equiv [A, [A, ..., [A, B]...]]$ is a commutator with A taken n times. It is worth noting that this series may be written in a simple closed form,

$$D = \frac{\int_0^F dF' \langle e^{i\mathcal{H}_2 F'/\hbar} j_z(0) e^{-i\mathcal{H}_2 F'/\hbar} j_z(0) \rangle}{\langle S(0)^2 \rangle},$$ (3.42)

which shows that our system is approximately equivalent to one with purely flip-flop interaction, evolving for a finite time, F.

61

3.5 Analytic Results

In this section we give analytic expressions for the diffusion coefficients to the two leading orders using Eq. (3.36) and Eq. (3.40). In order to make a comparison with the experiments on calcium fluoride, we specialize to the case of dipolar coupling, for which $A_{ij} = b_{ij}$, $B_{ij} = -\frac{1}{2}b_{ij}$, with b_{ij} given by Eq. (1.2). To obtain these analytic expressions we must evaluate infinite-temperature averages over products of spin operators. The evaluation of such averages is discussed in Appendix A.

3.5.1 Magnetization Diffusion

The denominator of Eq. (3.22) for $S = \mathcal{M}$ at $T = \infty$ is

$$\int d^3\mathbf{r} \int d^3\mathbf{r}' \langle \mathcal{M}(\mathbf{r}, 0)\mathcal{M}(\mathbf{r}', 0)\rangle = \frac{N\gamma^2\hbar^2}{4}. \tag{3.43}$$

The lowest order term is calculated exactly, by inserting the expressions for the Hamiltonian, Eq. (3.33), and the magnetization current, Eq.(3.31), into the first line of Eq. (3.36), and applying the identity, Eq. (3.38). We obtain

$$D_{\mathcal{M}}^{(0)} = \frac{1}{4}\sum_i z_{ik}^2 b_{ik}^2 F_{ik}, \tag{3.44}$$

$$z_{ij} \equiv z_i - z_j, \tag{3.45}$$

where F_{ij} is given by Eq. (3.41) with $G_{ij}(t)$ replacing $G(t)$. This result is identical to LGK's, as expected from the equivalence of the two methods.

The next term, obtained from Eq. (3.40) using all of the approximations discussed in the last section, is

$$D_M^{(2)} = -\frac{1}{4}\frac{F^3}{3!}\sum_{i,j} z_{ik}^2 b_{ik}^2 b_{jk}^2. \tag{3.46}$$

3.5.2 Energy Diffusion

For $S = \mathcal{H}$, the denominator is

$$\int d^3\mathbf{r} \int d^3\mathbf{r}' \langle \mathcal{H}(\mathbf{r}, 0)\mathcal{H}(\mathbf{r}', 0)\rangle = \frac{3}{16}\sum_i b_{ik}^2. \tag{3.47}$$

The lowest order term is

$$\begin{aligned}
D_{\mathcal{H}}^{(0)} &= \frac{1}{48\left(\sum_{i,j(i\neq j)} b_{ij}^2\right)} \left(\sum_{i,j,k} \left(b_{il}^2 b_{ik}^2 z_{kl}^2 + 8b_{il}^2 b_{kl}^2 z_{ik}^2 + 8b_{il}b_{ik}^2 b_{kl}z_{kl}z_{il} - 8b_{il}b_{ik}b_{kl}^2 z_{ik}z_{il} \right) F_{kl} \right. \\
&\quad \left. - \sum_{i,j,k,l} \left(8b_{ik}b_{jk}b_{kl}^2 z_{il}z_{jl} - 8b_{il}b_{jk}b_{kl}^2 z_{ik}z_{jl} + 8b_{jl}b_{ik}b_{jk}b_{kl}z_{il}z_{kl} + b_{il}b_{jl}b_{ik}b_{jk}z_{kl}^2 \right) R_{kl;ij} \right),
\end{aligned} \tag{3.48}$$

where

$$\begin{aligned}
R_{kl;ij} &\equiv \int_0^\infty dt\, K_{kl;ij}(t), \tag{3.49} \\
K_{kl;ij}(t) &\equiv -4\,\mathrm{tr}\,\{I_{iz}I_{jz}L_{kl}(t)\}|_{i\neq j\neq k\neq l} \\
&= \sin(\Delta_{kl;i}t)\sin(\Delta_{kl;j}t) \prod_{p(p\neq i,j,k,l)} \cos(\Delta_{kl;p}t), \tag{3.50} \\
\Delta_{kl;p} &\equiv b_{pk} - b_{pl}. \tag{3.51}
\end{aligned}$$

It is useful to have approximate analytic expressions for the integrals in Eq. (3.41) and Eq. (3.49). It has been shown that the saddle point approximation to F_{ij} is quite accurate.[25, 26] It is equivalent to replacing G_{ij} in the integrand by a gaussian,

$$G_{ij}(t) \approx \exp\left(-\frac{1}{2}\sum_{k(k\neq i,j)} (b_{ki} - b_{kj})^2 t^2\right). \tag{3.52}$$

To evaluate $R_{kl;ij}$, we replace the product of cosines in $K_{kl;ij}(t)$ by a gaussian, as above. Since this gaussian cuts off the integral at times $t \ll \hbar/b$, where b is of the order of the nearest neighbor coupling strength, we can expand the sine terms around

63

$t = 0$, which yields

$$K_{kl;ij}(t) \approx (b_{ik} - b_{il})(b_{jk} - b_{jl})t^2$$

$$\times \exp\left(-\frac{1}{2}\sum_{p(p\neq i,j,k,l)}(b_{pk} - b_{pl})^2 t^2\right), \qquad (3.53)$$

These approximations give

$$F_{ij} = \frac{\sqrt{\pi}}{\sqrt{2\sum_{k(k\neq i,j)}(b_{ki} - b_{kj})^2}}, \qquad (3.54)$$

$$R_{kl;ij} = \sqrt{\frac{\pi}{2}}\frac{(b_{ik} - b_{il})(b_{jk} - b_{jl})}{\left(\sum_{p(p\neq i,j,k,l)}(b_{pk} - b_{pl})^2\right)^{3/2}}. \qquad (3.55)$$

Eq. (3.54) has been derived previously.[25, 26] Eqs. (3.54) and (3.55) allow a more rapid numerical evaluation of the expressions for the diffusion coefficients than by numerical integration of Eqs. (3.39) and (3.50). By numerical integration on cubic lattices of between 5^3 and 11^3 spins, we have verified that Eq. (3.54) approximates the exact value with an error that is less than 2% and Eq. (3.55) approximates the exact value to within 10%.

We found numerically that the sum over R terms in Eq. (3.48) was about $20 - 25\%$ in magnitude of the sum over F terms, for both the (001) and (111) directions. The R terms arise from the lowest order (in I_{iz} operators) q-number correction to the approximation, Eq. (3.39), to $L_{ij}(t)$. We therefore expect this same number to also be a good estimate of the error in this approximation.

Using Eq. (3.40) for the next order term, we obtain

$$D_{\mathcal{H}}^{(2)} = \frac{F^3}{(3!)(192)\sum_{k,l}b_{kl}^2}\left(\sum_{u,q,l}\left(8b_{uq}^2 B_{uql}^2 + 4b_{uq}b_{lq}B_{qul}B_{qlu}\right)\right.$$

$$+ \sum_{u,q,l,k}\left[-b_{uq}^2\left(4B_{ukl}^2 + 2B_{kul}^2\right) + 4b_{uq}b_{kq}\left(B_{ukl}B_{luk} + 3B_{ulq}B_{qlk} + B_{uql}B_{lqk} - B_{uql}B_{luk}\right)\right.$$

$$\left.\left.- b_{qk}b_{ul}\left(4B_{ulk}B_{qkl} + 6B_{ukl}B_{qlk}\right)\right]\right), \qquad (3.56)$$

$$B_{ukl} \equiv b_{uk}b_{kl}z_{ul} + 2b_{uk}b_{ul}z_{kl} + 2b_{ul}b_{kl}z_{uk}. \tag{3.57}$$

3.6 Numerical Results

Because Eqs. (3.44), (3.46), (3.48), and (3.56) can be evaluated numerically only for finite lattice sizes, we use finite size scaling to extract the infinite lattice limit, as we did in section 2.3. The approach to the infinite lattice value is expected to follow a power law. A least squares fit to a power law was found to describe the scaling very well. For diffusion of magnetization, we were able to vary the lattice size, in increments of 2 lattice sites, between 1 and 81 lattice sites on an edge. For energy diffusion, we studied lattices with up to 27 sites on an edge.

The constant F in Eqs. (3.46), (3.56) was taken as the mean value of the F_{ij} over three layers of nearest neighbors. This averaging procedure works well since contributions for far-apart indices are suppressed by the b factors in the summations. In dimensionless units, this gave

$$\frac{\gamma^2 \hbar}{a^3} \times F = \begin{cases} 0.48 \pm 0.05, & (001) \text{ direction,} \\ 1.17 \pm 0.14, & (111) \text{ direction.} \end{cases} \tag{3.58}$$

The error, taken to be one standard deviation from the mean, is 10% for the (001) direction and 12% for the (111) direction. Therefore, the error in F^3 is about three times as much, or between 30% and 40%. As the magnitude of the second order terms is between 10% and 20% that of the zero order terms, the overall error in approximating $F_{ij} \approx F$ is less than 10%.

The results, including errors due to fitting and approximations, are summarized in Table 3.1. Our magnetization diffusion coefficient agrees well with experimental values. However, the energy diffusion coefficient that we obtain is several times smaller than observed experimentally, and is nearly the same as the magnetization diffusion coefficient. The relative orientation dependence is within the experimental range for magnetization, but disagrees drastically for energy.

65

Table 3.1: Summary of the theoretical results for the spin diffusion rate of energy, $D_{\mathcal{H}}$, and magnetization, $D_{\mathcal{M}}$ for a single crystal of calcium fluoride, using the hydrodynamic approach. These values have been obtained by numerically evaluating Eqs. (3.48) and (3.56), and Eqs. (3.44) and (3.46), using Eq. (3.54) for F_{ij} and Eq. (3.55) for R_{ikmj}. We used finite size scaling to extrapolate to the infinite lattice limit. Experimental results from Refs. [1, 2] are shown for comparison.

Theory		[001]	[111]	D_{001}/D_{111}
$D_M^{(0)}$	$(\times 10^{-12} \mathrm{cm}^2/\mathrm{s})$	8.4 ± 0.2	7.9 ± 0.2	–
$D_M^{(2)}$	$(\times 10^{-12} \mathrm{cm}^2/\mathrm{s})$	-1.1 ± 0.6	-1.0 ± 0.5	–
$D_M^{(0+2)}$	$(\times 10^{-12} \mathrm{cm}^2/\mathrm{s})$	7.3 ± 0.8	6.9 ± 0.7	1.1 ± 0.2
$D_{\mathcal{H}}^{(0)}$	$(\times 10^{-12} \mathrm{cm}^2/\mathrm{s})$	16.0 ± 0.6	11.9 ± 0.3	–
$D_{\mathcal{H}}^{(2)}$	$(\times 10^{-12} \mathrm{cm}^2/\mathrm{s})$	-2.5 ± 1.2	-2.3 ± 1.3	–
$D_{\mathcal{H}}^{(0+2)}$	$(\times 10^{-12} \mathrm{cm}^2/\mathrm{s})$	13.5 ± 1.8	9.6 ± 1.6	1.4 ± 0.4
Experiment, D_M		[001]	[111]	D_{001}/D_{111}
Ref. [2] $(\times 10^{-12} \mathrm{cm}^2/\mathrm{s})$		7.1 ± 0.5	5.3 ± 0.3	1.34 ± 0.12
Ref. [1] $(\times 10^{-12} \mathrm{cm}^2/\mathrm{s})$		6.4 ± 0.9	4.4 ± 0.5	1.45 ± 0.26
Experiment, $D_{\mathcal{H}}$		[001]	[111]	D_{001}/D_{111}
Ref. [1] $(\times 10^{-12} \mathrm{cm}^2/\mathrm{s})$		29 ± 3	33 ± 4	0.88 ± 0.14

3.7 Summary

We have presented a hydrodynamic approach to study the long-wavelength spin dynamics in a lattice of spins in high magnetic field and at high temperature. The Kubo formula, Eq. (3.22), for the diffusion coefficients applies to the physical regime probed experimentally and rests on the assumption that the time evolution of the system is ergodic. We developed a perturbation theory for Eq. (3.22) that is equivalent to the approach of LGK but simplifies the calculations enormously. This allowed us to obtain the diffusion coefficients for magnetization as well as energy to leading order in the flip-flop term of the Hamiltonian, and estimate the first perturbative correction. The result for magnetization diffusion agrees with experiment to within its degree of accuracy. The result for inter-spin energy diffusion is larger than that for magnetization diffusion, in qualitative agreement with the experiment. It does not, however, describe the experiment quantitatively.

One possible reason for the disparity is the ergodicity assumption, which is implicit

in our choice of how to take the average in the correlation functions appearing in Eq. (3.22). Our assumption of Eq. (3.8) leads to the equivalence of the non-equilibrium average of the conserved density to its equilibrium correlation function, as is usual in linear response theory.[43] For magnetization diffusion, the low polarization results in a very low density of polarized spins in a completely randomly polarized background. The sparsity of polarized spins means that their effect on each other is negligible, and they can be treated as independent. This suggests that statistical averaging over a complete infinite temperature ensemble is the correct procedure. For energy diffusion, the correlations inherent to the initial states used in the experiments of Boutis et al. may require the use of an ensemble that is a subset of the full Hilbert space. This would imply a modification of Eq.(3.8) for the density matrix at finite time, and needs to be investigated further.

The most evident source of inaccuracy in our calculation is our truncation of the perturbation series. Our estimate of the next-to-leading order correction to energy diffusion does not rule out the possibility that a resummation of our perturbation series would explain the experiment quantitatively. However, currently available non-perturbative (e.g. Bennet and Martin[24]) and resummation (e.g. Borckmans and Walgraef[27, 29]) methods are much too cumbersome to treat the diffusion of inter-spin energy. They are also plagued by their own uncontrolled approximations, such as the ad-hoc replacement of certain correlation functions by gaussians in order to simplify the calculations. This state of affairs, coupled with the great success of LGK at predicting the magnetization diffusion coefficient based on an expansion in the flip-flop term, and earlier that of Lowe and Norberg[40] at fitting the resonance lineshape by a similar expansion, motivated us to systematize their approach and apply it to inter-spin energy diffusion. For the final word on this problem, we await either a new non-perturbative method or a tractable technique for summing our perturbation series to all orders.

Appendix A

Diagrammatic technique for expectation values of spin operators

The diagrammatic technique is a useful bookkeeping device for easing the labor involved in evaluating equilibrium averages over products of spin operators. Its utility lies in eliminating the need to keep track of the products of Kronecker deltas that appear in a straightforward calculation of expectation values, as well as obviating any restrictions on the associated summations over lattice indices. The technique was introduced by Brout, Englert, Horwitz, and Stinchcombe[36, 37, 38, 39] (see also Ref. [50] for a pedagogical introduction) for the calculation of finite-temperature, static expectation values, such as equal-time correlation functions. They showed that such expectation values can be represented in terms of cluster expansions of connected diagrams. In this Appendix, we develop the technique for infinite-temperature expectation values of dynamical quantities, such as correlation functions at different times, and prove the cancellation of disconnected diagrams in this case. The combined case of dynamics at finite temperature is a simple extension of these methods.

We will be interested in evaluating averages over the infinite temperature equilib-

rium ensemble of products of spin operators of the type

$$T = \langle \mathcal{H}^n A_1 \mathcal{H}^m A_2 \rangle, \tag{A.1}$$

where the angular brackets represent the normalized trace, $\langle \cdots \rangle = \mathrm{tr}\{\cdots\}/\mathrm{tr}\{1\}$. Here $\mathcal{H}$ is the Hamiltonian of the spin system and A_1 and A_2 consist of spin operators. For instance, we could have $A_1 = I_i^z$, $A_2 = I_j^z$, for some indices i and j, as in Chapter 2, section 2.2.1. Expressions of this sort arise in the expansion of correlation functions like

$$C(t) = \frac{\langle e^{i\mathcal{H}t} A_1 e^{-i\mathcal{H}t} A_2 \rangle}{\langle A_1 A_2 \rangle}, \tag{A.2}$$

in powers of t or $\mathcal{H}$. We note that, as in Eq. (3.42) of Chapter 3, the "time" t may actually be a small parameter that has nothing to do with physical time.

For the remainder of this Appendix, we assume a Hamiltonian of the form of Eq. (2.14), which we reproduce here for convenience.

$$\mathcal{H} = \sum_{i,j} B_{ij} I_i^+ I_j^- \tag{A.3}$$

The more general Hamiltonian, Eq. (1.1), introduces nothing new. We can then write Eq. (A.1) as

$$T = \sum_{ijkl\ldots pq} B_{ij} B_{kl} \ldots B_{pq} \langle I_i^+ I_j^- I_k^+ I_l^- \ldots A_1 \ldots I_p^+ I_q^- \ldots A_2 \rangle, \tag{A.4}$$

with 2n spin operators to the left of A_1 and 2m to the right. The order is important because of the non-trivial commutation relations of the spin operators.

A.1 Ordered cumulants

We focus on averages of spin operators such as the term in brackets in Eq. (A.4). Such expressions must contain the same number of raising and lowering operators to be non-zero, which implies that we should only consider A_1 and A_2 with this property.

The non-zero elements of a spin operator average contain, in general, several instances of the same index on different operators. Operators with different indices commute, so that we may rearrange them to have all operators with the same index next to each other, and then factor the average into averages over operators at different lattice sites, since traces at different lattice sites are independent. For example, an expression such as $(1 - \delta_{ik})\langle I_k^+ I_i^z I_k^- I_i^z\rangle$ can be written $(1 - \delta_{ik})\langle I_k^+ I_k^- I_i^z I_i^z\rangle = (1 - \delta_{ik})\langle I^+ I^-\rangle_k \langle I^z I^z\rangle_i$. We will not write the indices on the averages from now on because the trace does not depend on them. Expressions such as Eq. (A.4) may be calculated by grouping the operators by index in this fashion, in all possible ways, taking care to avoid over-counting by not including identical groupings more than once.

We illustrate the statements in the preceding paragraph by considering a simple example. Suppose we are interested in evaluating $\langle I_i^z I_k^+ I_l^-\rangle$. Ignoring for the moment the fact that $\mathrm{tr}\,\{I_i^\alpha\} = 0 \ \forall \ i, \ \alpha$, we have

$$
\begin{aligned}
\langle I_i^z I_k^+ I_l^-\rangle \ &= \ \delta_{ikl}\langle I^z I^+ I^-\rangle + \delta_{ik}(1 - \delta_{ikl})\langle I^z I^+\rangle\langle I^-\rangle \\
&\quad + \delta_{il}(1 - \delta_{ikl})\langle I^z I^-\rangle\langle I^+\rangle + \delta_{kl}(1 - \delta_{ikl})\langle I^+ I^-\rangle\langle I^z\rangle \\
&\quad + (1 - \delta_{ik})(1 - \delta_{il})(1 - \delta_{kl})\langle I^z\rangle\langle I^+\rangle\langle I^-\rangle,
\end{aligned}
\tag{A.5}
$$

where the δ symbols are zero unless all their indices are the same, and ensure that each distinct term is counted only once. It simplifies matters to regroup the terms in Eq. (A.5) according to the δ symbols, as follows.

$$
\begin{aligned}
\langle I_i^z I_k^+ I_l^-\rangle \ &= \ \delta_{ikl}\left(\langle I^z I^+ I^-\rangle - \langle I^z I^+\rangle\langle I^-\rangle - \langle I^z I^-\rangle\langle I^+\rangle \right.\\
&\quad \left. - \langle I^+ I^-\rangle\langle I^z\rangle + 2\langle I^z\rangle\langle I^+\rangle\langle I^-\rangle\right) \\
&\quad + \delta_{ik}\left(\langle I^z I^+\rangle - \langle I^z\rangle\langle I^+\rangle\right)\langle I^-\rangle \\
&\quad + \delta_{il}\left(\langle I^z I^-\rangle - \langle I^z\rangle\langle I^-\rangle\right)\langle I^+\rangle \\
&\quad + \delta_{kl}\left(\langle I^+ I^-\rangle - \langle I^+\rangle\langle I^-\rangle\right)\langle I^z\rangle. \\
&\quad + \langle I^z\rangle\langle I^+\rangle\langle I^-\rangle.
\end{aligned}
\tag{A.6}
$$

To analyze this expression further, we introduce ordered cumulants of spin op-

erators, also known as semi-invariants,[36] which are related to the averages of spin operators in a similar way to the relation between moments and cumulants of a statistical distribution in probability theory. (See, e.g. Ref. [51].) They may be defined as the distinct elements of the factorization of a product of spin operators into all possible partitions respecting the original order of the operators. Using a double angular bracket to distinguish cumulants from averages, we define

$$
\begin{aligned}
\langle I^z I^+ I^- \rangle &\equiv \langle\langle I^z I^+ I^- \rangle\rangle + \langle\langle I^z I^+ \rangle\rangle\langle\langle I^- \rangle\rangle + \langle\langle I^z I^- \rangle\rangle\langle\langle I^+ \rangle\rangle + \langle\langle I^+ I^- \rangle\rangle\langle\langle I^z \rangle\rangle \\
&\quad + \langle\langle I^z \rangle\rangle\langle\langle I^+ \rangle\rangle\langle\langle I^- \rangle\rangle, \\
\langle I^z I^+ \rangle &\equiv \langle\langle I^z I^+ \rangle\rangle + \langle\langle I^z \rangle\rangle\langle\langle I^+ \rangle\rangle, \\
\langle I^z I^+ \rangle &\equiv \langle\langle I^z I^+ \rangle\rangle + \langle\langle I^z \rangle\rangle\langle\langle I^+ \rangle\rangle, \\
\langle I^z I^- \rangle &\equiv \langle\langle I^z I^- \rangle\rangle + \langle\langle I^z \rangle\rangle\langle\langle I^- \rangle\rangle, \\
\langle I^+ I^- \rangle &\equiv \langle\langle I^+ I^- \rangle\rangle + \langle\langle I^+ \rangle\rangle\langle\langle I^- \rangle\rangle, \\
\langle I^z \rangle &\equiv \langle\langle I^z \rangle\rangle, \\
\langle I^+ \rangle &\equiv \langle\langle I^+ \rangle\rangle, \\
\langle I^- \rangle &\equiv \langle\langle I^- \rangle\rangle.
\end{aligned}
$$

$$\text{(A.7)}$$

From this the method for defining ordered cumulants of any number of spin operators should be clear. These equations may be inverted to obtain each ordered cumulant of a given degree iteratively in terms of averages of equal or lower degree. This gives

$$
\begin{aligned}
\langle\langle I^z I^+ \rangle\rangle &= \langle I^z I^+ \rangle - \langle I^z \rangle\langle I^+ \rangle, \\
\langle\langle I^z I^- \rangle\rangle &= \langle I^z I^- \rangle - \langle I^z \rangle\langle I^- \rangle, \\
\langle\langle I^+ I^- \rangle\rangle &= \langle I^+ I^- \rangle - \langle I^+ \rangle\langle I^- \rangle, \\
\langle\langle I^z I^+ I^- \rangle\rangle &= \langle I^z I^+ I^- \rangle - \langle I^z I^+ \rangle\langle I^- \rangle - \langle I^z I^- \rangle\langle I^+ \rangle - \langle I^+ I^- \rangle\langle I^z \rangle \\
&\quad + 2\langle I^z \rangle\langle I^+ \rangle\langle I^- \rangle.
\end{aligned}
$$

$$\text{(A.8)}$$

The expressions on the right hand side are the same as those in parentheses in Eq.

Table A.1: Ordered Cumulants for spin 1/2. We use the shorthand notation + for I^+, $-$ for I^-, and z for I^z. Cumulants that do not have the same number of raising and lowering operators are zero, and are not included. We also include only one of each set of cumulants that differ by a cyclic permutation of its operators. As discussed in the text, these cumulants are the same.

$\langle\langle z \rangle\rangle$	$= 0$		$\langle\langle + - + - z \rangle\rangle$	$= 0$
$\langle\langle zz \rangle\rangle$	$= \frac{1}{4}$		$\langle\langle - + + - z \rangle\rangle$	$= 0$
$\langle\langle +- \rangle\rangle$	$= \frac{1}{2}$		$\langle\langle + - - + z \rangle\rangle$	$= 0$
$\langle\langle + - z \rangle\rangle$	$= \frac{1}{4}$		$\langle\langle + + - - z \rangle\rangle$	$= -\frac{1}{2}$
$\langle\langle - + z \rangle\rangle$	$= -\frac{1}{4}$		$\langle\langle - - + + z \rangle\rangle$	$= \frac{1}{2}$
$\langle\langle zzz \rangle\rangle$	$= 0$		$\langle\langle - + - + z \rangle\rangle$	$= 0$
$\langle\langle zzzz \rangle\rangle$	$= -\frac{1}{8}$		$\langle\langle + + + - - - \rangle\rangle$	$= \frac{3}{2}$
$\langle\langle + - zz \rangle\rangle$	$= 0$		$\langle\langle + + - + - - \rangle\rangle$	$= \frac{1}{2}$
$\langle\langle +z - z \rangle\rangle$	$= -\frac{1}{4}$		$\langle\langle + + - - + - \rangle\rangle$	$= \frac{1}{2}$
$\langle\langle + - +- \rangle\rangle$	$= \frac{1}{2}$		$\langle\langle + - + - + - \rangle\rangle$	$= \frac{1}{2}$
$\langle\langle + + -- \rangle\rangle$	$= -\frac{1}{2}$			

(A.6). This is not an accident, since the cumulant of a given degree is found by subtracting from the average its successive factorizations into cumulants of lower degree, which is just what was done when we regrouped the terms in going from Eq. (A.5) to Eq. (A.6).

A list of ordered cumulants up to degree 5 for spin $\frac{1}{2}$ is given in Table A.1. We omit cumulants that differ only by a cyclic permutation of their operators, since these are the same by the properties of the trace. Besides cyclic permutations, cumulants differing by any other rearrangements in the order of the operators generally have different values.

We may now write Eq. (A.6) in the concise form,

$$\langle I_i^z I_k^+ I_l^- \rangle = \delta_{ikl}\langle\langle I^z I^+ I^- \rangle\rangle + \delta_{ik}\langle\langle I^z I^+ \rangle\rangle\langle\langle I^- \rangle\rangle + \delta_{il}\langle\langle I^z I^- \rangle\rangle\langle\langle I^+ \rangle\rangle$$

$$+\delta_{kl}\langle\langle I^+ I^- \rangle\rangle\langle\langle I^z \rangle\rangle + \langle\langle I^z \rangle\rangle\langle\langle I^+ \rangle\rangle\langle\langle I^- \rangle\rangle. \qquad (A.9)$$

If we are interested in a sum of the form $\sum_{ikl} Q_{ikl}\langle I_i^z I_k^+ I_l^- \rangle$, we find that each term in Eq. (A.9) gives rise to an unrestricted summation of the coefficient, Q_{ikl}, multiplied by a product of cumulants, over the independent indices determined by these cumulants. For example, the second term of Eq. (A.9) gives

$$\langle\langle I^z I^+ \rangle\rangle\langle\langle I^- \rangle\rangle \sum_{il} Q_{iil}. \qquad (A.10)$$

A.2   Diagrammatic technique

Returning now to Eq. (A.4), we may evaluate it by partitioning the average into cumulants in all possible ways, each cumulant receiving the index of the operators it contains, and then summing over the distinct indices. With each summation index we associate a point in space, called a vertex, and with each operator inside the cumulant corresponding to a given vertex we associate a diagram element connected to this vertex. A possible choice for the diagram elements for the different spin operators is as follows

$$I^z \longrightarrow \bigcirc \qquad (A.11)$$

$$I^+ \longrightarrow \qquad (A.12)$$

$$I^- \longrightarrow \qquad (A.13)$$

Here I^+ is represented by a directed line leaving a vertex, I^- is represented by a directed line entering a vertex, and I^z is represented by a circle. The cumulant
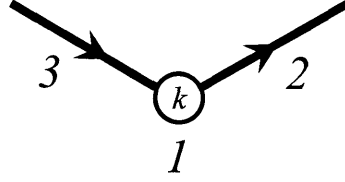
Figure A-1: Diagram representing the cumulant $\langle\langle I^z I^+ I^- \rangle\rangle$ with index k.

$\langle\langle I^z I^+ I^- \rangle\rangle$ with index k is then represented by the diagram in Fig. A-1. We have numbered the diagram elements in this figure to indicate the order in which the operators appear in the cumulant. (Note, for instance, that $\langle\langle I^+ I^z I^- \rangle\rangle \neq \langle\langle I^z I^+ I^- \rangle\rangle$.)

Because of the presence of the coefficients B_{ij} in Eq. (A.4), with the property $B_{ii} = 0$, we associate a special diagram with the Hamiltonian, namely

$$\mathcal{H} \longrightarrow \quad \text{\large$\updownarrow$} \tag{A.14}$$

where lines corresponding to the raising and lowering operators are connected, but the vertices cannot be joined.

We can now associate a set of diagrams to Eq. (A.1) according to the following rules. To the $n+m$ operators $\mathcal{H}$ there correspond $n+m$ interaction diagram elements as in Eq. (A.14). To the operators A_1, A_2 correspond diagram elements assembled from the ones in Eqs. (A.11) - (A.13). The vertices belonging to spin operators in A_1, A_2 must be distinguished in some way from those of the interaction lines, because they have different coefficients associated with them. In Chapter 2 this is done by using open circles, as for the I^z diagram. These diagram elements are then numbered according to the order in which they appear in Eq. (A.1). Next, the diagram elements are joined at vertices in all topologically distinct ways. To each vertex corresponds an ordered cumulant, and to each interaction line corresponds a coupling constant, B_{ij}. To each line or circle belonging to A_1 or A_2 corresponds the appropriate coefficient, if there is one. The analytic expression for a given diagram is found by taking the product of the cumulants, coupling constants, and coefficients from A_1 and A_2 that are
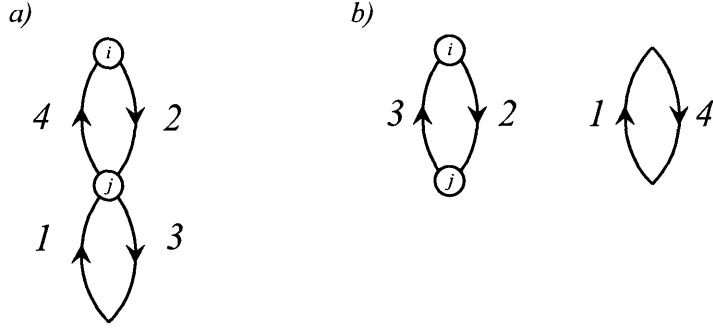
Figure A-2: Two diagrams contributing to Eq. (A.1) for $n = 1$, $m = 1$, $A_1 = \frac{1}{2} \sum_k B_{ik} I_i^+ I_k^-$, $A_2 = \frac{1}{2} \sum_l B_{jl} I_j^+ I_l^-$. a) is connected and b) is disconnected.

associated with that diagram. The entire average in Eq. (A.1) is found by summing the analytic expressions from all the different diagrams corresponding to it.

We note that there can be both connected and disconnected diagrams. One example of each is shown in Fig. A-2 for the case $n = 1$, $m = 1$, $A_1 = \frac{1}{2} \sum_k B_{ik} I_i^+ I_k^-$, $A_2 = \frac{1}{2} \sum_l B_{jl} I_j^+ I_l^-$. This particular choice occurs in the evaluation of the second moment for the energy autocorrelation function in Chapter 2. The analytic values associated with these diagrams are

$$T(a) = \langle\langle + - \rangle\rangle^2 \langle\langle + + - - \rangle\rangle \left(\frac{1}{2}\right)^2 \sum_k B_{ij}^2 B_{jk}^2 = -\frac{1}{32} \sum_k B_{ij}^2 B_{jk}^2, \quad (A.15)$$

$$T(b) = \langle\langle + - \rangle\rangle^4 \left(\frac{1}{2}\right)^2 \sum_{kl} B_{ij}^2 B_{kl}^2, \quad (A.16)$$

where we have used the shorthand notation and values for the cumulants in Table A.1. If we are interested in correlation functions of the form of Eq. (A.2), it turns out that disconnected diagrams do not contribute, and we are left with a linked cluster expansion. We show how this comes about in the next section.

A.3 Cancellation of disconnected diagrams

Because the applications we are interested in are limited to the case where the interaction Hamiltonian is time-independent, we present a proof of the cancellation of disconnected diagrams for the correlation function, Eq. (A.2), based on a commutator expansion in the Heisenberg picture. In the case of Hamiltonians more complicated than Eq. (A.3), it is possible to proceed by the standard method via the interaction picture and S-matrix expansion.[52] However, the lack of a Wick-type theorem for spin operators prohibits the factorization of time-ordered products into contractions, and we must eventually use the same type of counting argument presented here. (We do use an interaction representation in Chapter 3. However, the time dependence of the interaction Hamiltonian there is only a c-number factor, allowing us to proceed in the fashion described here.)

By the same steps as as were used in going from Eq. (2.1) to Eq. (2.3) and then to Eq. (2.16), we rewrite Eq. (A.2) as

$$C(t) = \frac{1}{\langle A_1 A_2 \rangle} \sum_{n=0}^{\infty} \left(\frac{it}{n!}\right)^n \sum_{m=0}^{n} \left(\begin{array}{c} n \\ m \end{array}\right) (-1)^m \langle \mathcal{H}^{n-m} A_1 \mathcal{H}^m A_2 \rangle. \tag{A.17}$$

There are two types of disconnected diagrams, those in which both A_1 and A_2 appear in the same cumulant, and those in which they belong to different cumulants. The latter type of disconnected diagram is always zero, because the cyclic permutation symmetry of the trace allows us to factor all the cumulants to the left of the summation over m in Eq. (A.17).

The case where both A_1 and A_2 appear in the same cumulant is slightly more involved. Consider the subset of diagrams for which $l < n$ interaction lines form the part which is not connected to that containing A_1 and A_2. For example, $l = 2$ in diagram b) of Fig. A-2. The l interaction lines can correspond to any of the n $\mathcal{H}$'s appearing in Eq. (A.17), whose average may be factored outside the summation over m. Depending on which ones we choose to factor out, there will be a different number of $\mathcal{H}$'s to the right of the operator A_1. If we choose to leave $k < n$ $\mathcal{H}$'s to the right

77

of A_1, we can do this in $\begin{pmatrix} m \\ m-k \end{pmatrix} \begin{pmatrix} n-m \\ l-(m-k) \end{pmatrix}$ ways. The sum over m in Eq. (A.17) for set of diagrams with l $\mathcal{H}$'s factored out is therefore equal to

$$
\sum_{m=0}^{n} \begin{pmatrix} n \\ m \end{pmatrix} (-1)^m \langle \mathcal{H}^{n-m} A_1 \mathcal{H}^m A_2 \rangle
$$

$$
= \langle \mathcal{H}^l \rangle \sum_{k=0}^{n-l} \langle \mathcal{H}^{n-l-k} A_1 \mathcal{H}^k A_2 \rangle \sum_{m=k}^{l+k} (-1)^m \begin{pmatrix} n \\ m \end{pmatrix} \begin{pmatrix} m \\ m-k \end{pmatrix} \begin{pmatrix} n-m \\ l-(m-k) \end{pmatrix}.
$$
$$(A.18)$$

The product of binomial coefficients in this equation is

$$
\begin{pmatrix} n \\ m \end{pmatrix} \begin{pmatrix} m \\ m-k \end{pmatrix} \begin{pmatrix} n-m \\ l-(m-k) \end{pmatrix} = \frac{n!m!(n-m)!}{(n-m)!m!(m-k)!k!(l+k-m)!(n-l-k)!}
$$

$$
= \frac{n!}{(m-k)!k!(l+k-m)!(n-l-k)!}. \qquad (A.19)
$$

The only factors that depend on m are $\frac{1}{(m-k)!(l+k-m)!} = \frac{1}{l!} \begin{pmatrix} l \\ m-k \end{pmatrix}$. The sum over m in Eq. (A.18) is therefore $\sum_{m=k}^{l+k} (-1)^m \begin{pmatrix} l \\ m-k \end{pmatrix} = 0$. This proves the vanishing of disconnected diagrams.

Appendix B

Diagrams contributing to fourth moment for energy

In the table beginning on the following page are listed all the diagrams and corresponding analytic expressions contributing to the fourth moment for energy. This moment is given by Eq. (2.16) with $n = 2$,

$$M_S^{(4)} = \frac{(-1)^{n+1}k^2}{2\sum_i \text{tr}\{S_i(0)^2\}} \sum_{i,j} z_{ij}^2 \sum_{m=0}^{4} \binom{4}{m} (-1)^m \text{tr}\{\mathcal{H}^m S_j(0)\mathcal{H}^{4-m}S_i(0)\}. \quad \text{(B.1)}$$

In this equation we take $S_i(0) = \sum_k \mathcal{H}_{ik}$, with $\mathcal{H}_{ik}$ given in Eqs. (2.26) –(2.28), which we reproduce here for convenience.
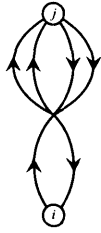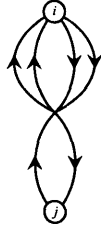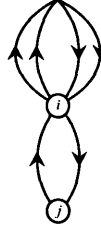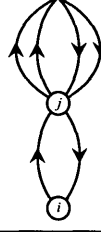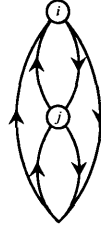
$$\mathcal{H}_{ik} = \mathcal{H}_{ik}^{(+)} + \mathcal{H}_{ik}^{(-)}, \quad \text{(B.2)}$$
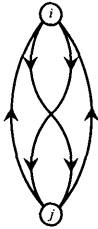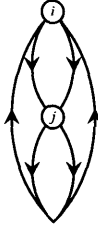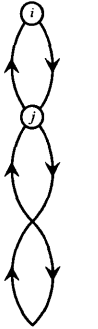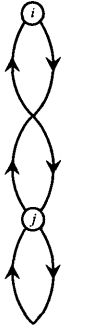
$$\mathcal{H}_{ik}^{(+)} \equiv \frac{1}{2}B_{ik}I_i^+ I_k^-, \quad \text{(B.3)}$$

$$\mathcal{H}_{ik}^{(-)} \equiv \frac{1}{2}B_{ik}I_i^- I_k^+, \quad \text{(B.4)}$$
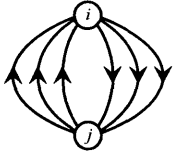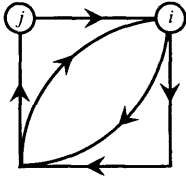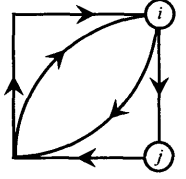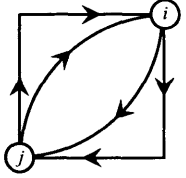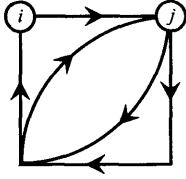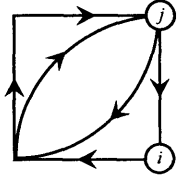
Table B.1: All topologically distinct diagrams with six interaction lines and two circles, along with corresponding analytic expressions, for Eq. (B.1) with $S_i(0) = \sum_k \mathcal{H}_{ik}$. We note that the calculation in section 2.2.2 was set up in such a way that i and j were not treated symmetrically in the intermediate steps (see Eqs. (2.29) – (2.31)). Because the diagrams below were calculated from Eq. (2.29), some of them do not have the same value when these indices are interchanged.
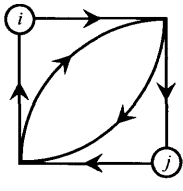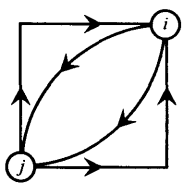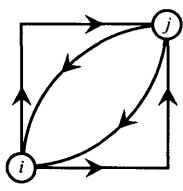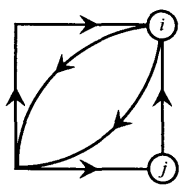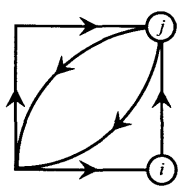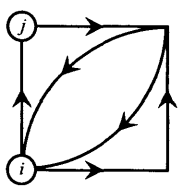
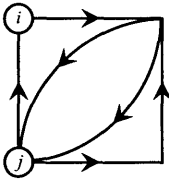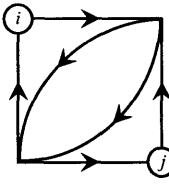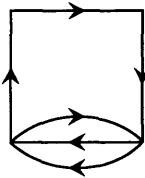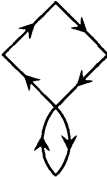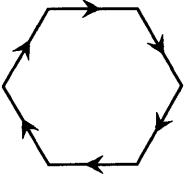| Diagram	Analytic Expression
	0
	0
	$\dfrac{k^2 \sum_{ijkl} z_{ij}^2 B_{ik}^2 B_{jk}^2 B_{kl}^2}{\sum_{kl} B_{kl}^2}$
	0
	0

Diagram	Analytic Expression
	$-\dfrac{k^2 \sum_{ijk} z_{ij}^2 B_{ik}^4 B_{jk}^2}{\sum_{kl} B_{kl}^2}$
	$-\dfrac{k^2 \sum_{ijk} z_{ij}^2 B_{ik}^2 B_{jk}^4}{\sum_{kl} B_{kl}^2}$
	0
	0
	$-\dfrac{k^2 \sum_{ijk} z_{ij}^2 B_{ij}^2 B_{ik}^2 B_{jk}^2}{\sum_{kl} B_{kl}^2}$

Diagram	Analytic Expression
	$-\dfrac{5}{4}\dfrac{k^2\sum_{ijk}z_{ij}^2 B_{ij}^2 B_{ik}^2 B_{jk}^2}{\sum_{kl}B_{kl}^2}$
	$\dfrac{5}{2}\dfrac{k^2\sum_{ijk}z_{ij}^2 B_{ij}^2 B_{ik}^2 B_{jk}^2}{\sum_{kl}B_{kl}^2}$
	$\dfrac{1}{2}\dfrac{k^2\sum_{ijkl}z_{ij}^2 B_{ij}^2 B_{jk}^2 B_{kl}^2}{\sum_{kl}B_{kl}^2}$
	$\dfrac{1}{4}\dfrac{k^2\sum_{ijkl}z_{ij}^2 B_{ik}^2 B_{jk}^2 B_{jl}^2}{\sum_{kl}B_{kl}^2}$

Diagram	Analytic Expression
	$-\dfrac{1}{2}\dfrac{k^2\,\Sigma_{ijkl}\,z_{ij}^2 B_{ik}^2 B_{jl}^2 B_{kl}^2}{\Sigma_{kl}\,B_{kl}^2}$
	$-\dfrac{1}{2}\dfrac{k^2\,\Sigma_{ijkl}\,z_{ij}^2 B_{ij}^2 B_{ik}^2 B_{jl}^2}{\Sigma_{kl}\,B_{kl}^2}$
	$\dfrac{1}{4}\dfrac{k^2\,\Sigma_{ijkl}\,z_{ij}^2 B_{ik}^2 B_{il}^2 B_{jk}^2}{\Sigma_{kl}\,B_{kl}^2}$
	$\dfrac{1}{2}\dfrac{k^2\,\Sigma_{ijkl}\,z_{ij}^2 B_{ij}^2 B_{ik}^2 B_{kl}^2}{\Sigma_{kl}\,B_{kl}^2}$

Diagram	Analytic Expression
	0
	$\dfrac{1}{2}\dfrac{k^2 \Sigma_{ijkl}\, z_{ij}^2 B_{ij} B_{ik}^2 B_{il} B_{jk} B_{kl}}{\Sigma_{kl}\, B_{kl}^2}$
	$\dfrac{1}{4}\dfrac{k^2 \Sigma_{ijkl}\, z_{ij}^2 B_{ij} B_{ik}^2 B_{il} B_{jk} B_{kl}}{\Sigma_{kl}\, B_{kl}^2}$
	$-\dfrac{1}{2}\dfrac{k^2 \Sigma_{ijkl}\, z_{ij}^2 B_{ij}^2 B_{ik} B_{il} B_{jk} B_{jl}}{\Sigma_{kl}\, B_{kl}^2}$
	$\dfrac{1}{4}\dfrac{k^2 \Sigma_{ijkl}\, z_{ij}^2 B_{ij} B_{ik} B_{jk}^2 B_{jl} B_{kl}}{\Sigma_{kl}\, B_{kl}^2}$
	$\dfrac{1}{2}\dfrac{k^2 \Sigma_{ijkl}\, z_{ij}^2 B_{ij} B_{ik} B_{jk}^2 B_{jl} B_{kl}}{\Sigma_{kl}\, B_{kl}^2}$

Diagram	Analytic Expression
	$$-\frac{7}{4}\frac{k^2\sum_{ijkl}z_{ij}^2 B_{ik}B_{il}B_{jk}B_{jl}B_{kl}^2}{\sum_{kl}B_{kl}^2}$$
	$$\frac{1}{2}\frac{k^2\sum_{ijkl}z_{ij}^2 B_{ij}^2 B_{ik}B_{il}B_{jk}B_{jl}}{\sum_{kl}B_{kl}^2}$$
	$$-\frac{3}{2}\frac{k^2\sum_{ijkl}z_{ij}^2 B_{ij}^2 B_{ik}B_{il}B_{jk}B_{jl}}{\sum_{kl}B_{kl}^2}$$
	$$\frac{k^2\sum_{ijkl}z_{ij}^2 B_{ij}B_{ik}^2 B_{il}B_{jk}B_{kl}}{\sum_{kl}B_{kl}^2}$$
	$$\frac{3k^2\sum_{ijkl}z_{ij}^2 B_{ij}B_{ik}B_{jk}^2 B_{jl}B_{kl}}{\sum_{kl}B_{kl}^2}$$
	$$\frac{1}{2}\frac{k^2\sum_{ijkl}z_{ij}^2 B_{ij}B_{ik}^2 B_{il}B_{jk}B_{kl}}{\sum_{kl}B_{kl}^2}$$

Diagram	Analytic Expression
	$$-\frac{3}{2}\frac{k^2\sum_{ijkl}z_{ij}^2 B_{ij}B_{ik}B_{jk}^2 B_{jl}B_{kl}}{\sum_{kl}B_{kl}^2}$$
	$$-\frac{k^2\sum_{ijkl}z_{ij}^2 B_{ik}B_{il}B_{jk}B_{jl}B_{kl}^2}{\sum_{kl}B_{kl}^2}$$
	0 for all diagrams of this type
	0 for all diagrams of this type
	0 for all diagrams of this type
	0 for all diagrams of this type

86

Bibliography

[1] G. S. Boutis, D. Greenbaum, H. Cho, D. G. Cory, and C. Ramanathan. *Phys. Rev. Lett.*, 92:137201, 2004.

[2] W. Zhang and D. G. Cory. *Phys. Rev. Lett.*, 80:1324, 1998.

[3] D. Greenbaum, M. Kindermann, C. Ramanathan, and D. G. Cory. cond-mat/0401013, unpublished.

[4] W.-K. Rhim, A. Pines, and J. S. Waugh. *Phys. Rev. B*, 3:684, 1971.

[5] A. Abragam. *Principles of Nuclear Magnetism*. Oxford, New York, 1961.

[6] H. A. Reich. *Phys. Rev.*, 129:630, 1963.

[7] E. R. Hunt and J. R. Thompson. *Phys. Rev. Lett.*, 20:249, 1968.

[8] J. M. Taylor, G. Giedke, H. Christ, B. Paredes, J. I. Cirac, P. Zoller, M. D. Lukin, and A. Imamoglu. cond-mat/0407640. unpublished.

[9] J. M. Taylor, C. M. Marcus, and M. D. Lukin. *Phys. Rev. Lett.*, 90:206803, 2003.

[10] M. Eto, T. Ashiwa, and M. Murata. *J. Phys. Soc. Jpn.*, 73:307, 2004.

[11] R. G. Mani, W. B. Johnson, and V. Narayanamurti. Proceedings of 15th International Conference on the Application of High Magnetic Fields in Semiconductor Physics, Oxford, 5-9 August 2002, Institute of Physics Conference Series Number 171, edited by A. R. Long and J. H. Davies (IOP, Bristol, 2003) 1.6.

[12] A. V. Sologubenko, S. M. Kazakov, H. R. Ott, T. Asano, and Y. Ajiro. *Phys. Rev. B*, 68:094432, 2003.

[13] C. P. Slichter. *Principles of Magnetic Resonance*. Springer-Verlag, Berlin, third edition, 1996.

[14] N. Bloembergen. *Physica*, 15:386, 1949.

[15] J. H. Van Vleck. *Phys. Rev.*, 74:1168, 1948.

[16] J. Jeener and P. Broekaert. *Phys. Rev.*, 139:1959, 1965.

[17] D. K. Sodickson and J. S. Waugh. *Phys. Rev. B*, 52:6467, 1995.

[18] G. R. Khutsishvili. *Sov. Phys.-JETP*, 4:382, 1957.

[19] P. G. DeGennes. *J. Phys. Chem. Solids*, 7:345, 1958.

[20] A. G. Redfield. *Phys. Rev.*, 116:315, 1959.

[21] W. E. Blumberg. *Phys. Rev.*, 119:79, 1950.

[22] M. Goldman. *Phys. Rev.*, 138:A1675, 1965.

[23] L. L. Buishvili and D. N. Zubarev. *Fizika Tverdogo Tela*, 7:722, 1965. [English translation: *Sov. Phys. - Solid State*, 7:580, (1965).].

[24] H. S. Bennett and P. C. Martin. *Phys. Rev.*, 138:A608, 1965.

[25] I. J. Lowe and S. Gade. *Phys. Rev.*, 156:817, 1967.

[26] J. I. Kaplan. *Phys. Rev. B*, 2:4578, 1970.

[27] P. Borckmans and W. Walgraef. *Phys. Rev.*, 167:282, 1968.

[28] A. G. Redfield and W. N. Yu. *Phys. Rev.*, 169:443, 1968. Erratum: *Phys. Rev.* 177:1018, 1969.

[29] P. Borckmans and W. Walgraef. *Physica*, 68:157, 1973.

[30] C. Tang and J. S. Waugh. *Phys. Rev. B*, 45:748, 1992.

[31] S. Sachdev and K. Damle. *Phys. Rev. Lett.*, 78:943, 1997.

[32] K. Damle and S. Sachdev. *Phys. Rev. B*, 57:8307, 1998.

[33] B. N. Narozhny, A. J. Millis, and N. Andrei. *Phys. Rev. B*, 58:R2921, 1998.

[34] K. Fabricius and B. M. McCoy. *Phys. Rev. B*, 57:8340, 1998.

[35] E. B. Fel'dman and M. G. Rudavets. *Chem. Phys. Lett.*, 311:453, 1999.

[36] R. Brout. *Phys. Rev.*, 115:824, 1959.

[37] R. Brout. *Phys. Rev.*, 118:1009, 1960.

[38] F. Englert. *Phys. Rev.*, 129:567, 1963.

[39] R. B. Stinchcombe, G. Horwitz, F. Englert, and R. Brout. *Phys. Rev.*, 115:824, 1959.

[40] I. J. Lowe and R. E. Norberg. *Phys. Rev.*, 107:46, 1957.

[41] G. B. Furman and S. D. Goren. *J. Phys.-Condens. Matter*, 11:4045, 1999.

[42] G. B. Furman and S. D. Goren. *Phys. Rev. B*, 68:064402, 2003.

[43] D. Forster. *Hydrodynamic Fluctuations, Broken Symmetry, and Correlation Functions*. Perseus Books, 1975.

[44] J. S. Waugh. *Mol. Phys.*, 95:731, 1998.

[45] E. B. Fel'dman and S. Lacelle. *J. Chem. Phys.*, 108:4709, 1998.

[46] E. B. Fel'dman, R. Brüschweiler, and R. R. Ernst. *Chem. Phys. Lett.*, 294:297, 1998.

[47] H. M. Pastawski and G. Usaj. *Phys. Rev. B*, 57:5017, 1998.

[48] B. V. Fine. *Int. J. Mod. Phys. B*, 18:1119, 2004.

[49] G. B. Furman. private communication.

[50] A. Abragam and M. Goldman. *Nuclear Magnetism: Order and Disorder*. Clarendon, Oxford, 1982.

[51] Eric W. Weisstein. "Cumulant". From MathWorld–A Wolfram Web Resource. http://mathworld.wolfram.com/Cumulant.html.

[52] M. E. Peskin and D. V. Schroeder. *An Introduction to Quantum Field Theory*. Perseus Books, 1995.